SJCE

SCIENTIFIC JOURNAL OF CIVIL ENGINEERING

EDITORIAL - Preface to Volume 6 Issue 1 of the Scientific Journal of Civil Engineering (SJCE)

Todorka Samardzioska EDITOR – IN - CHIEF

Dear Readers,

Scientific Journal of Civil Engineering (SJCE) was established in December 2012. It is published bi-annually and is available online at the web site of the Faculty of Civil Engineering in Skopje (www.gf.ukim.edu.mk).

This Journal welcomes original works within the field of civil engineering, which includes: all the types of engineering structures and materials, water engineering, geo-technics, highway and railroad engineering, survey and geo-spatial engineering, buildings and environmental protection, construction management and many others. The Journal focuses on analysis, experimental work, theory, practice and computational studies in the fields.

The international editorial board encourages all researchers, practitioners and members of the academic community to submit papers and contribute for the development and maintenance of the quality of the SJCE journal.

As an editor of the Scientific Journal of Civil Engineering (SJCE), it is my pleasure to introduce the First Issue of VOLUME 6. The primary goal continues to be high quality of publications, enhancing objectivity and fairness of the review process.

This issue includes five articles in the field of modelling and testing of different building materials, cartographic conic projection and estimation of prices of real estates. The first paper explains a new material model of externally bonded FRP strips and sheets, used for strengthening and repair of shear walls. The second paper provides information of modified testing of the properties of shear connectors, while the basic elementary calculation of conformal conic projection with two standard parallels applied on the territory of Republic of Macedonia is explained in detail in the third paper.

Physical and mechanical properties of the concrete made with variable quantity of processed waste glass aggregates are presented in the fourth article. Finally, the fifth paper investigates the sensitivity of dilation angle on numerical simulation of reinforced concrete (RC) deep beams.

Wishing you nice summer and successful completion of the academic year!

Sincerely Yours,

Prof. Dr. Sc. Todorka Samardzioska

July, 2017

SJCE

SCIENTIFIC JOURNAL OF CIVIL ENGINEERING

Impressum

CONTENTS

Become a student of the Faculty of Civil Engineering and a part of the impetus that creates and build the world! Step in the world of the successful people, because even the longest roads start with the first step. You will spend a part of your youth with us, and the youth is expensive to be misspent in vain. Your choice is an exceptional profession, for people who do believe in themselves, profession that requires prompt and courageous decisions. This profession will provide you with great privileges: your actions will remain an eternal record in the space and in the time being.

- STRUCTURAL ENGINEERING
- HYDRO-TECHNICAL ENGINEERING
- ROADS AND RAILWAYS ENGINEERING
- GEODESY
- GEOTECHNICAL ENGINEERING

LT978.

SS CYRIL AND METHODIUS UNIVERSITY
FACULTY OF CIVIL ENGINEERING
gf.ukim.edu.mk

AUTHOR

Vladimir Vitanov

Ph.D. Associated Professor
University Ss. Cyril and Methodius
Faculty of Civil Engineering –Skopje
v.vitanov@gf.ukim.edu.mk

MATERIAL MODEL OF FRP STRENGTHENED REINFORCED CONCRETE IN BIAXIAL STRESS STATE SUBJECTED TO MONOTONIC LOADING CONDITIONS

The application of shear walls as a primary earthquake resistant mechanism in structural design is traditionally accepted and used over the last decades. However, very often, older structures having shear walls no longer comply with the contemporary standards and codes which raise the need for their strengthening and retrofit. Many strengthening measures and techniques have been designed and used. One of the newest and most promising is the use of externally bonded FRP strips and sheets. Intensive research has started in order to design the most economic and efficient technique for application of these materials. Different modelling approaches have been employed in these designs. This paper presents the attempt to formulate a new material model that could be used to model FRP strengthened RC member and its implementation into ANSYS. The model results are tested against the available experimental data in order to verify its correctness and practical usability. The obtained results show satisfactory match when compared with the experimental data.

Keywords: Finite Element Method (FEM), ANSYS, reinforced concrete, strengthening, FRP

1. INTRODUCTION

The conventional earthquake resistant design of reinforced concrete structures advises use of shear walls as effective way to add earthquake resistance to the reinforced concrete frames. A problem arises with structures erected decades ago following design rules which are by today's standards obsolete, inadequate and inefficient. Major earthquake events from around the world have shown the design deficiencies of these structures by inducing extensive damages in the structural members. Many of the old shear wall buildings are at risk of suffering damages from a major earthquake mostly due to their insufficient in-

plane stiffness, flexural and shear strengths and ductility owing to the older design codes which didn't adequately estimate the demands that major earthquakes impose on the structures. This problem is ever increasing as the existing structures are getting older and their members gradually deteriorate.

Many different methods of seismic strengthening and repair of shear wall structures have been developed and tested in the last thirty years. Recently, state-of-the-art strengthening and retrofit techniques increasingly utilize externally bonded fiber reinforced polymer (FRP) composites, which offer unique properties in terms of strength, lightness, chemical resistance, and ease of application. Such techniques are most attractive for their fast execution and low labor costs.

Only recently have researchers attempted to simulate the behavior of reinforced concrete strengthened with FRP composites using the finite element method. The majority of the studies that included numerical modeling of FRP strengthened RC members with FEM use element overlaying, where one-, two- or even three dimensional elements (solid or layered) that represent the FRP material are superimposed over the concrete elements, either with (ex. Khomwan and Foster [7]; Wong and Vecchio [12]) or without (ex. Kheyroddin and Naderpour [6]) interface elements that represent the influence of the adhesive material or the bond between the FRP and the concrete.

A different approach is presented in this paper. An attempt is made to formulate a new material model which will simplify the modeling of FRP strengthened reinforced concrete members. The newly formulated material model is implemented into ANSYS [1] and tested using available experimental data.

2. MODEL FORMULATION

In the analysis of RC structures plane stress problems make up a large majority of practical cases. Therefore, the numerical model presented here is based on the inelastic model for cyclic biaxial loading of reinforced concrete of Darwin and Pecknold [3] which was designed to be used for such type of structures (shear walls, beams, slabs, shear panels, shells, reactor containment vessels).

2.1 CONCRETE

The concrete is treated as incrementally linear, elastic material, which means that during each load increment the material is assumed to behave elastically. It is also considered to exhibit stress-induced orthotropic material behavior. The constitutive relationship for incrementally linear orthotropic material with reference to the principal axes of orthotropy can be written as:

$$\begin{Bmatrix} d\sigma_1 \\ d\sigma_2 \\ d\tau_{12} \end{Bmatrix} = D_C \begin{Bmatrix} d\varepsilon_1 \\ d\varepsilon_2 \\ d\gamma_{12} \end{Bmatrix} \tag{1}$$

with D_C being:

$$D_C = \frac{1}{1-v^2} \begin{bmatrix} E_1 & v\sqrt{E_1 E_2} & 0 \\ v\sqrt{E_1 E_2} & E_2 & 0 \\ 0 & 0 & (1-v^2)G \end{bmatrix} \tag{2}$$

where $d\sigma_i$ and $d\varepsilon_i$ are the stress and strain increments, E_1 and E_2 are initial concrete stiffness modules in principal directions, $v = \sqrt{v_1 v_2}$ is the "equivalent" poison ratio, $G = \frac{1}{4(1-v^2)}(E_1 + E_2 - 2v\sqrt{E_1 E_2})$ is the shear modulus and D_C is the concrete constitutive matrix in the principle directions. Before it can be used in the finite element procedure, the concrete constitutive matrix is transformed to global coordinates using:

$$D_C' = T^T D_C T \tag{3}$$

where T is the strain transformation matrix (Cook, 1974). At the moment when the principle tensile stress exceeds the concrete tensile strength a "crack" forms perpendicular to the principle stress direction. This is modelled by reducing the values of E and v to zero. This has an effect of creating a "smeared" rather than discrete crack. The constitutive equation for the cracked concrete then takes the form:

$$\begin{Bmatrix} d\sigma_1 \\ d\sigma_2 \\ d\tau_{12} \end{Bmatrix} = \begin{bmatrix} 0 & 0 & 0 \\ 0 & E_2 & 0 \\ 0 & 0 & \dfrac{E_2}{4} \end{bmatrix} \begin{Bmatrix} d\varepsilon_1 \\ d\varepsilon_2 \\ d\gamma_{12} \end{Bmatrix} \tag{4}$$

If the tensile strength in the other principle direction is exceeded then a second crack occurs and the constitutive matrix is then reduced to $D_C = [0]$. In order to keep track of

the material degradation, the concept of "equivalent uniaxial strain" is used. It allows derivation of the actual biaxial stress-strain curves from uniaxial curves. The equation suggested by Saenz [10] is frequently used for this purpose:

$$\sigma_i = \frac{\varepsilon_{ui} \cdot E_0}{1 + \left(\dfrac{E_0}{E_S} - 2\right)\dfrac{\varepsilon_{ui}}{\varepsilon_{ci}} + \left(\dfrac{\varepsilon_{ui}}{\varepsilon_{ci}}\right)^2} \qquad (5)$$

where E_0 is the tangent modulus of elasticity at zero stress, E_S is the secant modulus at the point of maximum compressive stress (σ_{ci}), and ε_{ci} is the equivalent uniaxial strain at maximum compressive stress, Fig.1. The concrete biaxial strength envelope suggested by Kupfer and Gerstle [9], Fig. 2, is used to determine the value of σ_{ci}.
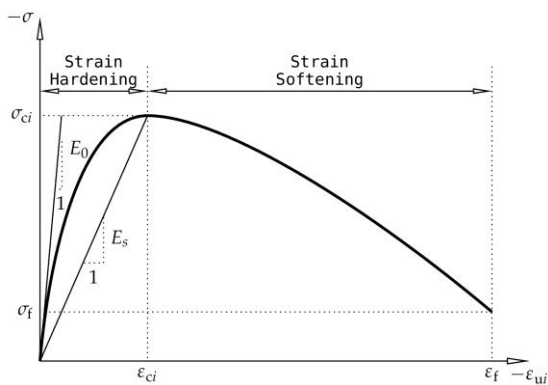
Figure 1. Equivalent Uniaxial Stress-Strain Curve in Compression [4].
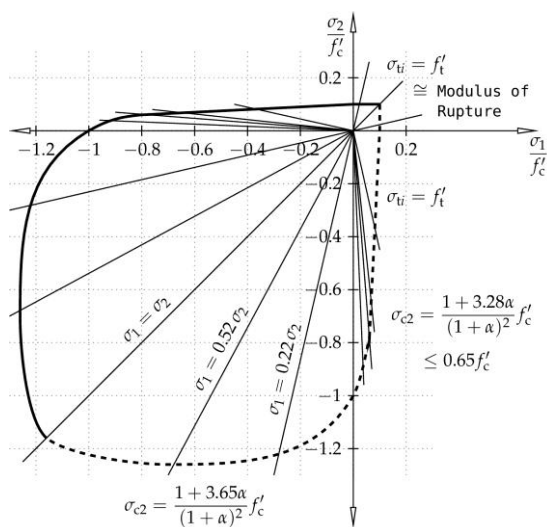
Figure 2. Analytical Biaxial Strength Envelope [9]

2.2 REINFORCING STEEL

Generally, the reinforcing steel can be modeled as discrete or distributed. The model presented here considers the reinforcing steel to be distributed, or "smeared", throughout the concrete. A simple, bilinear model with strain hardening is adopted for the stress-strain behavior of the steel. The constitutive matrix of the steel defined in the steel direction is

$$D_S = p_S \begin{bmatrix} E_{steel} & 0 & 0 \\ 0 & 0 & 0 \\ 0 & 0 & 0 \end{bmatrix} \qquad (6)$$

with E_{steel} the tangent stiffness of the steel and p_S the reinforcing ratio. Depending on the stress level in the steel, E_{steel} can be either equal to the initial steel stiffness E_S or reduced by a strain hardening stiffness ratio (δ), see Fig.3. Before using it in the composite material matrix, D_S is transformed to the global coordinates using the strain transformation matrix (T).
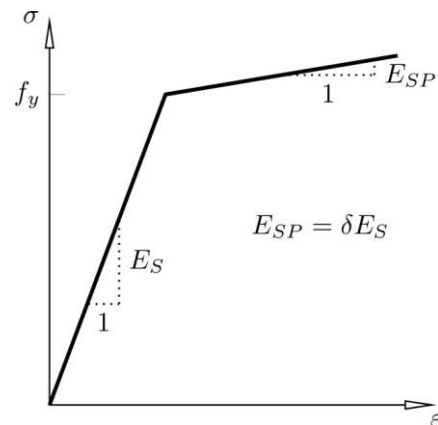
Figure 3. Stress-strain curve of reinforcing steel

2.3 FRP STRENGTHENING

The influence of the FRP strengthening is accounted for in the same fashion as the reinforcing steel. The material is treated as distributed, or "smeared" throughout the concrete. Its material behavior is assumed to be elastic-brittle, having abrupt failure after reaching its maximal strength (Fig.4). It is also capable of transmitting only tension stresses. The constitutive matrix of the FRP defined in the direction of the FRP fibers is therefore:

$$D_F = p_F \begin{bmatrix} E_F & 0 & 0 \\ 0 & 0 & 0 \\ 0 & 0 & 0 \end{bmatrix} \quad (7)$$

with E_F the tangent stiffness of the FRP and p_F the "strengthening" ratio. Before using it in the composite material matrix D_F must also transformed to the global coordinates using the strain transformation matrix (T).
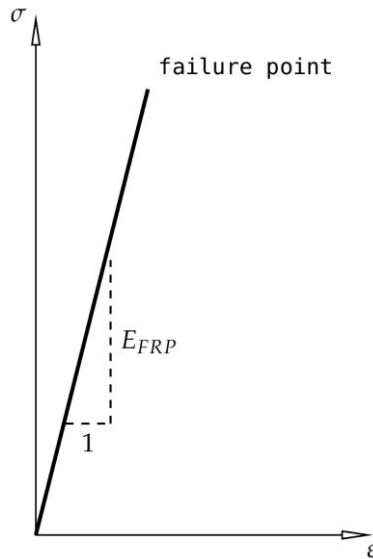
Figure 4. Stress-strain curve of FRP

2.4 COMPOSITE MATERIAL MATRIX

After defining the constitutive matrices of the constituent materials, the constitutive matrix of the composite material in the global coordinates is obtained by their summation:

$$D' = D_C' + \sum_{i=1}^{n} D_{S,i}' + \sum_{i=1}^{m} D_{F,i}' \quad (8)$$

where D', D_C', $D_{S,i}'$ and $D_{F,i}'$ are the constitutive matrices if the composite material, concrete, steel and FRP in global coordinates, respectively, n is the number of different reinforcing steels and m is the number of different FRPs used for strengthening.

3. VERIFICATION

The material model briefly described in the second section was coded and implemented into ANSYS in order to test its correctness and usability by comparing the results from numerical analyses with the available experimental data from the literature.

3.1 GARDEN AND HOLLAWAY (1998)

Garden and Hollaway [5] performed four point bending tests on 1 m long RC beams strengthened with CFRP. The CFRP plates with a thickness of 0.82 mm were attached to the soffit of the beam. The beam with designation $3_{U,1.0m}$ was analyzed here (Fig. 5). Three different sections or parts of the beam (top, bottom and middle) were defined in order to accommodate the steel reinforcement and FRP strengthening placement in the actual beam cross-section (Fig.6). Only half of the beam was model making use of the beam and load symmetry. The material properties for the reinforcing steel and the FRP strengthening for the three parts of the beam model are given in Table 1. The concrete definition for the whole beam was the same, having uniaxial compression strength of $f_C' = 43 \text{MPa}$, uniaxial tensile strength of $f_t' = 3 \text{MPa}$, initial modulus of elasticity $E_0 = 40 \text{GPa}$, equivalent uniaxial strain at maximum strength $\varepsilon_{cu} = -0.0022$ and equivalent Poisson's ratio $\nu = 0.2$.
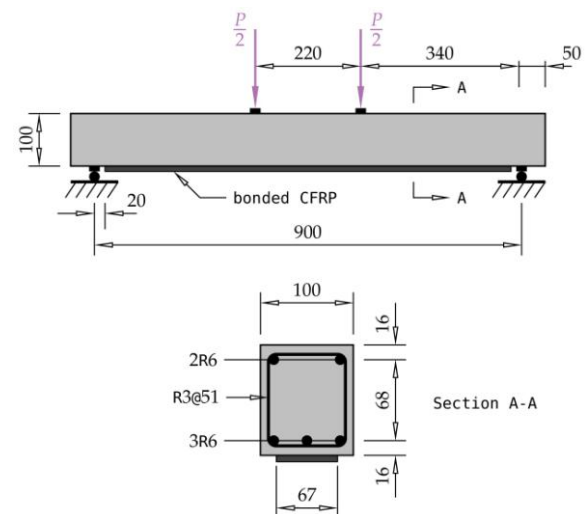
Figure 5. Test specimen $3_{U,1.0m}$[5]
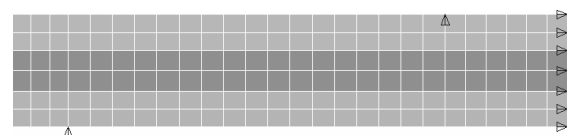
Figure 6. FEM model of test specimen $3_{U,1.0m}$ in ANSYS

Displacement control analysis was performed by applying series of vertical displacements at the point where the load was applied in the actual test. The obtained load-deflection curve

is shown in Fig. 7. While the beam stiffness in the initial load increments was apparently overestimated, the rest of the curve stays very close to the shape of the experimental curve.

Table 1. Material parameters for the $3_{U,1.0m}$ beam used in the analysis

| Part	Steel #1 (horizontal)			
	f_y	E_S	δ	p_S
	MPa	GPa	%	%
Bottom	350	215	0	2.7
Top	350	215	0	2.7
Middle	-	-	-	-
Part	Steel #2 (horizontal)			
Bottom	350	215	0	1.7
Top	350	215	0	1.7
Middle	350	215	0	1.7
Part	FRP			
	E_S		ε_F	p_F
	GPa		%	%
Bottom	110		1.2	1.7
Top	-		-	-
Middle	-		-	-
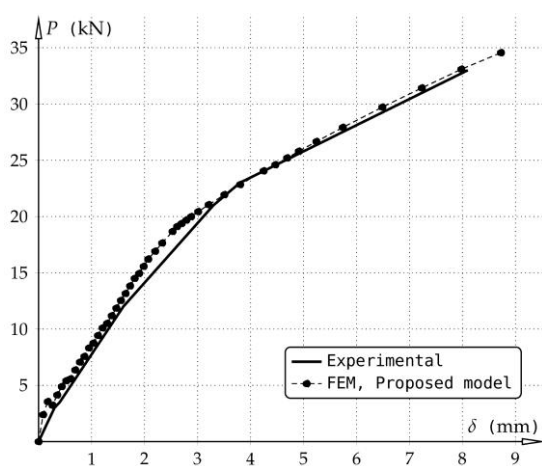
Figure 7. Load versus mid-span deflection of $3_{U,1.0m}$ beam

3.2 WONG (2001)

Wong [11] has conducted test on three large-scale beams. They were then analyzed by Wong and Vecchio [12]. The beams were designed with only tension reinforcement. No shear steel reinforcement was used. Instead, CFRP strips were glued to the side surfaces to act as shear strengthening. The geometry of the three beam specimens is shown in Fig. 8. The CFRP fabric used for strengthening was composed of graphite fibers oriented in the longitudinal direction and Kevlar 49 weft in the perpendicular direction. The material was tested to obtain its material properties. Tensile strength of 1090 MPa and ultimate strain of 0.011 were recorded. Strips of this material with a width of 200 mm were bonded on the side surfaces (not wrapped around the beam) at a central distance of 300 mm between each other. The beams were tested under monotonic three-point loading until failure.

In the FEM analyses performed by Wong and Vecchio [12], 2D elements were used to represent the concrete. The elements were double noded with one set of nodes used for the concrete elements, while the second set was used to attach the truss elements that represented the FRP. Then the coincident nodes were connected by contact or link elements representing the bond.

The finite element model used here was build using 4-node quadrilateral Plane182 elements. Only half of the each test specimen was modelled making use of its symmetry (Fig. 9). To properly model the longitudinal steel reinforcement, the beams were divided into two parts - upper and lower part, with the lower part being of height of 130 mm and containing the smeared longitudinal reinforcement. The material properties of the two parts for each of the beams are presented in Tables 2, 3 and 4. The available experimental data was used to calibrate the models. The resulting load-deflection curves are shown in Fig. 10. They are compared with the recorded experimental data as well as with the results of the FEM analysis performed by Wong and Vecchio [12]. It can be seen that the obtained results closely follow the experimental curves especially in the deflection range up to the steel yielding point. The failure in the models occurred due to concrete crushing at the top point in the symmetry axes, i.e. the location where the load is applied. The performed analyses showed different results in predicting the point of failure which was mostly influenced by the finite element and load step sizes.
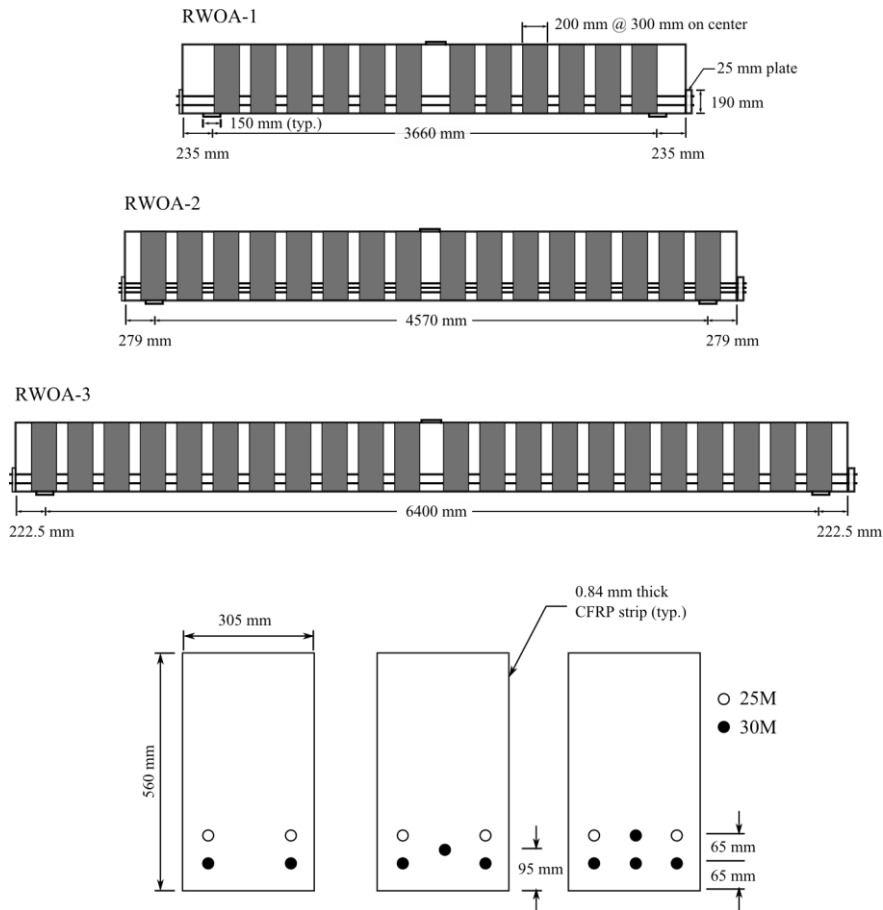
Figure 8. Elevation views and cross section details of RWOA beams [11]
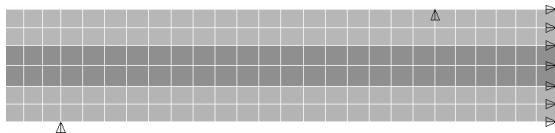
Figure 9. FEM mesh model of RWOA beams in ANSYS

Table 2. Material Parameters for the concrete of the RWOA Beams used in the Analysis

Beam	f'_C	E_0	f_t	ε_{cu}	ν
RWOA	MPa	GPa	MPa	%	%
1	23	18	4	-0.35	0.2
2	26	20	4	-0.35	0.2
3	44	25	4	-0.35	0.2

Table 3. Material Parameters for the steel in the lower part of the RWOA Beams, used in the Analysis (the upper part of the beams does not contain any steel material)

Beam	f_y	E_S	δ	p_S
RWOA	MPa	GPa	%	%
1	430	200	1	5.6
2	400	200	1	7.3
3	400	200	1	8.9

Table 4. Material Parameters for the FRP of the RWOA Beams used in the Analysis

Beam	E_0	ε_F	p_F
RWOA	GPa	%	%
1	100	1.1	0.2
2	100	1.1.	0.2
3	100	1.1	0.2
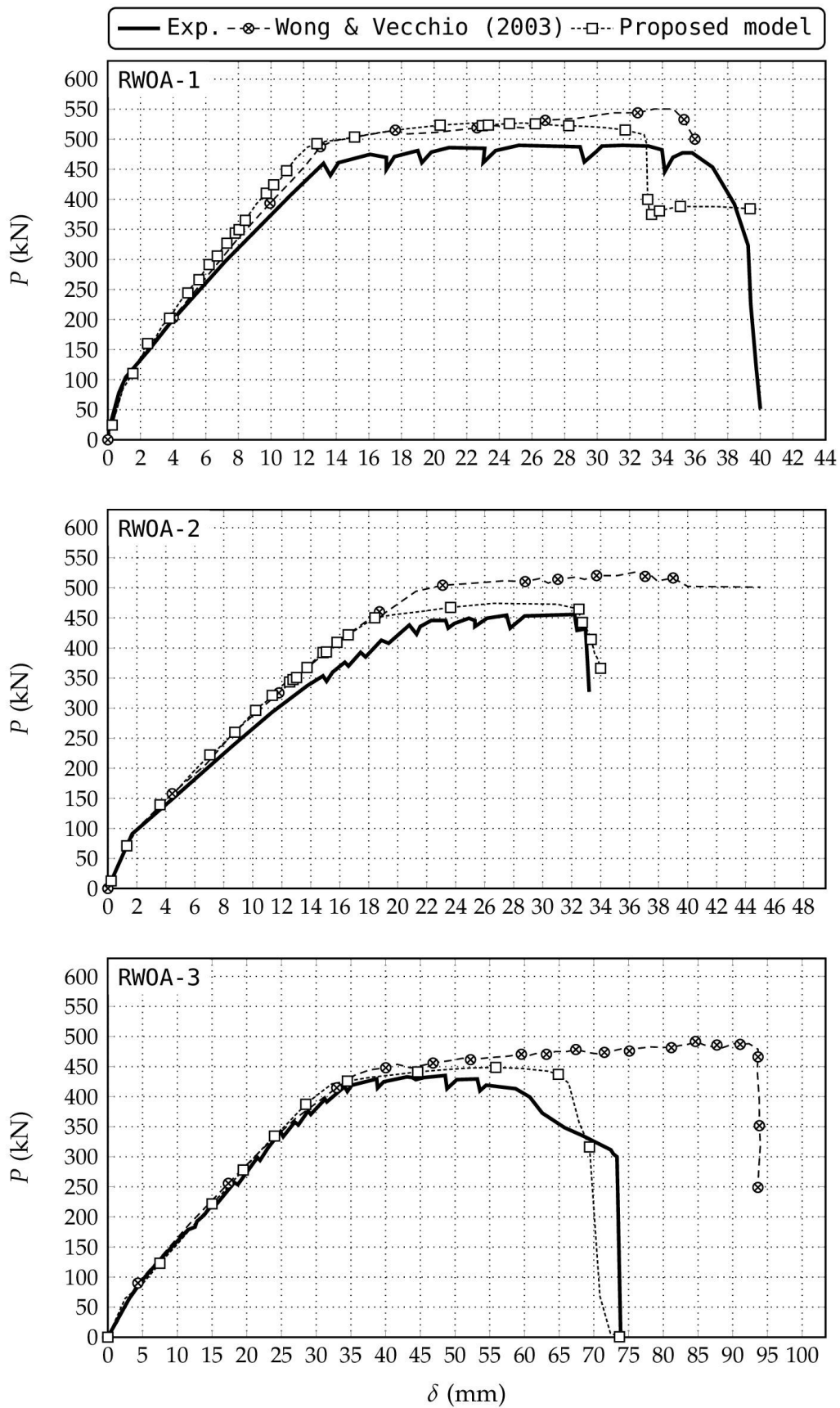
Figure 10. Load versus mid span deflection for RWOA beams [11]

4. SUMMARY AND CONCLUSIONS

The paper present an attempt to formulate material model which will correctly simulate the behavior of reinforced concrete members in plane stress strengthened with FRP materials. The presented model builds up on the concepts of an earlier model reinforced concrete model of Darwin and Pecknold. It uses the uniaxial strain approach in modelling of biaxially loaded reinforced concrete and the distributed approach of modelling the cracking behavior and the reinforcing steel.

The proposed model is subsequently implemented into the code of the general finite element method program ANSYS as a user material model in order to test its results against the available experimental data. Two different analyses were presented: An analysis of RC beam strengthened for bending by externally bonded FRP strips on the soffit side if the beam and analyses of three RC beams strengthened by externally bonded FRP wraps on their sides. The results are compared against the experimentally obtained data as well as against the numerical results from another finite element analysis performed by other authors employing more traditional approach into finite element modelling if such problems. Based on the presented results, it can be concluded that the proposed model is able to correctly simulate the behavior of the RC beams strengthened with FRP in different configurations. Its ANSYS implementation enables its use in both research and practical purposes, facilitating the further research in this field as well as the practical applications in the construction industry.

REFERENCES

[1]   ANSYS Inc., ANSYS®Multiphysics, Release 9.0

[2]   Cook, R. D. (1974). Concepts and applications of finite element analysis. New York: John Wiley & Sons.

[3]   Darwin, D. and Pecknold, D.A.W. (1974). Inelastic Model for Cyclic Loading of Reinforced Concrete, Civil Engineering Studies SRS-409, University of Illinois, Urbana Champaign, Illinois, 169 pages.

[4]   Hu, H.-T. and Schnobrich, W. C. (1989). Constitutive modeling of concrete by using nonassociated plasticity, *Journal of Materials in Civil Engineering*, 1, 199–216.

[5]   Garden, H. and Hollaway, L. (1998). An experimental study of the influence of plate end anchorage of carbon fibre composite plates used to strengthen reinforced concrete beams, *Composite Structures*, 42(2), 175–188.

[6]   Kheyroddin, A. & Naderpour, H. (2008). Nonlinear finite element analysis of composite RC shear walls, *Iranian Journal of Science & Technology, Transaction B, Engineering*, 32(B2), 79–89.

[7]   Khomwan, N. and Foster, S. J. (2004). Finite Element Modelling of FRP Strengthened Beams and Walls. Technical Report UNICIV Report R-432, The University of New South Wales, School of Civil and Environmental Engineering, Kensington, Sydney 2052 Australia, 68 pages.

[8]   Kupfer, H., Hilsdorf, H.K. and Rusch (1969). Behavior of Concrete Under Biaxial Stresses, *ACI Journal Proceedings*, 656-666.

[9]   Kupfer, H. and Gerstle, K.H. (1973). Behavior of Concrete Under Biaxial Stresses, *Journal of Engineering Mechanics Division*, 852-866.

[10] Saenz, L. (1964). Discussion of "Equation for Stress-Strain Curve of Concrete" by Desayi and Krishman, *ACI Journal*, 1229-1235

[11] Wong, R. S. Y. (2001). Towards modelling of reinforced concrete members with externally-bonded fibre reinforced polymer (FRP) composites. Master's thesis, University of Toronto, Toronto, Canada.

[12] Wong, R.S.Y. and Vecchio, F.J. (2003). Towards modeling of reinforced concrete members with externally bonded fiber-reinforced polymer composites. *ACI Structural Journal* **100:1**,47-55.

AUTHORS

Denis Popovski

PhD, Assistant professor

Ss. Cyril and Methodius University

Faculty of Civil Engineering – Skopje

Bul. Partizanski odredi No. 24, 1000 Skopje

popovski@gf.ukim.edu.mk

Mile Partikov

MSc, Assistant

Ss. Cyril and Methodius University

Faculty of Civil Engineering – Skopje

partikov@gf.ukim.edu.mk

Petar Cvetanovski

PhD, Full Professor

University "Ss. Cyril and Methodius"

Faculty of Civil Engineering – Skopje

cvetanovski@gf.ukim.edu.mk

MODIFIED TEST ON SHEAR CONNECTORS WITH PROFILED STEEL SHEETING TRANSVERSE TO THE BEAM

When the design rules are not applicable, the design can be based on tests, carried out in a way that provides information on the properties of the shear connection required for design [1].

Testing the shear connectors gives necessary relevant data revealing the real behaviour of the composite structure, and the capability of achieving the full plastic capacity of the designed cross section.

The modified testing, scope of this paper, is a part of a large experimental trials conducted for retrieving of larger volume of relevant data on the different behaviour of composite structures.

The modified testing on shear connectors is conducted on such way that represents the real behaviour of the composite structure, using three identical specific samples.

Keywords: composite structures, shear connectors, headed stud.

1. STANDARD TESTING

The rules for testing arrangements, preparation of specimens, testing procedure and test evaluation are given in EN 1994-1-1, Annex B, Part B.2.

1.1 TESTING ARRANGEMENTS AND PREPARATION

When the shear connectors are part of T-beam with uniform concrete slab, or with haunches, standard testing is used for determination of the behaviour of the shear connectors. In other cases, with use of profiled sheeting decks, longitudinal or transversal to the beam, modified test can be used.

For modified tests the dimensions and the arrangement of the parts that create the cross section must be as the designed, but in accordance of the rules given in EN 1994-1-1, Annex B, such as the length of each slab should be related to the longitudinal spacing of

the connectors. The width of each slab should not exceed the effective width of the slab of the beam. The thickness of each slab should not exceed the minimum thickness of the slab in the beam and the slabs should have the same haunch and reinforcements as the beam.
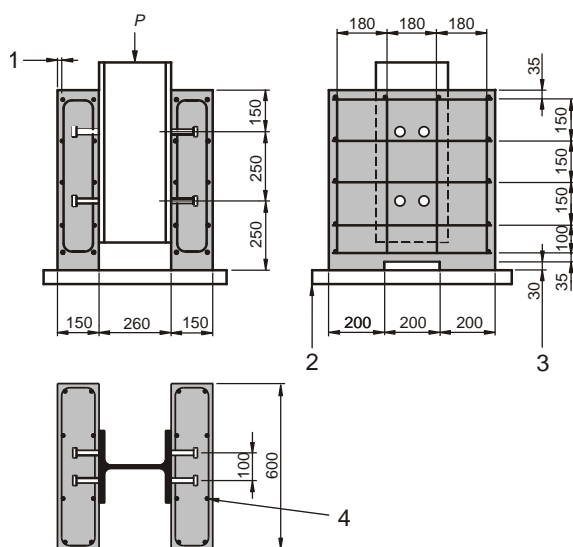

Figure 1. Test specimen for standard testing

Where 1) is cover of 15mm, 2) is bedding from mortar or gypsum, 3) is recess and it is optional and 4) is reinforcement ribbed bars and steel section.

The casting of the concrete slabs is in horizontal position, as for the real composite beam, and the specimen should be air-cured. For each mix of concrete minimum three specimens of cylinders or cubes should be prepared for determination of the concrete strength.

The yield strength and the maximum elongation of a representative sample of the shear connector material, steel beam, and steel sheeting should be determined.

1.2 TESTING PROCEDURE AND EVALUATION

The testing procedure is the same for the standard and for the modified tests. The load is applied in increments up to 40% of the expected failure load and cycled 25 times between 5% and 40%. After the cycled loading, subsequent load increment is imposed until failure occur in not less than 15 minutes. The longitudinal slip between the concrete and the steel section should be measured continuously until the load dropped to 20% below the maximum load. Also, the transverse separation between the steel

section and the concrete should be measured, closely to the groups of connectors.

If the results of the three specimens does not exceed 10%, the design resistance can be determined as follows:

- The characteristic resistance P_{rk} should be taken as the minimum failure load reduced by 10%

- The design resistance P_{rd} should be calculated as given in (1)

$$P_{Rd} = \frac{f_u \cdot P_{Rk}}{f_{ut} \cdot \gamma_v} \leq \frac{P_{Rk}}{\gamma_v} \qquad (1)$$

Where,

- f_u is the minimum specified ultimate strength of the connector material

- f_{ut} is the actual ultimate strength of the connector material in the specimen

- γ_v is the partial safety factor for shear connection

If the deviation from the main exceeds 10%, three more tests should be made, and the test evaluation should be carried in accordance with EN1990, Annex D.

The slip capacity δ_u is the maximum slip measured at the characteristic load level. The characteristic slip capacity δ_{uk} is the minimum test value of δ_u reduced by 10% or statistical evaluation from all the results in accordance with EN 1990, Annex D.

2. MODIFIED TESTING

The modified test sample is T-beam cross section with IPE270 as main steel beam, with transverse steel sheeting Bondeck 600 with stud shear connectors through deck welded with diameter d=19mm and height h_{sc}=100mm. The concrete slab thickness is 52+58=110mm, where 52mm is the height of the steel sheeting deck, and 58mm is the continuous concrete plate, reinforced with Q273 (Ø6/100mm), as shown in Figure 2. The concrete strength class is C25/30 according to EN 1992-1-1, Table 3.1.

At the top of the steel beam, detail for receiving the force is constructed, composed from steel plate 200x300x15mm and UNP100 profiles as stiffeners. The bottom face of the

concrete slab is bedded in mortar (exmal) with thickness approximately of 50mm.
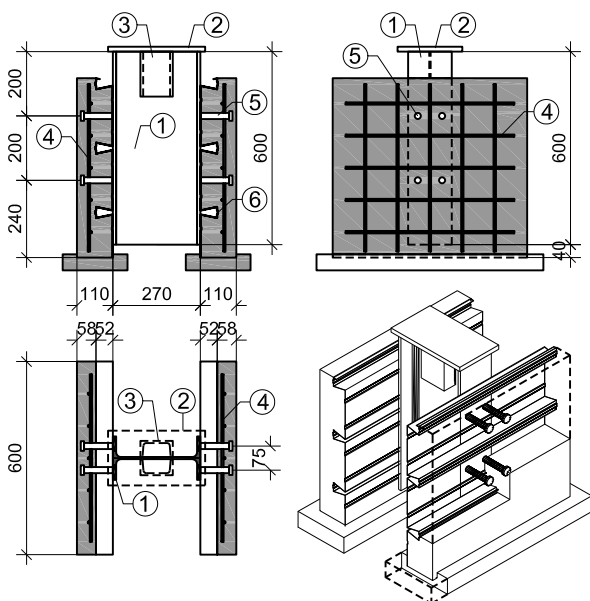

Figure 2. Test specimen for modified testing

Where, 1) is steel beam IPE200, 2) is steel plate 200x300x15, 3) is UNP100 as stiffeners, 4) is reinforcement Q283 (Ø6/100mm), 5) is headed stud type Nelson d=19mm, h_{sc}=100mm and 6) is steel sheeting Bondeck 600 t=1.0mm.

The casting of the concrete slabs was made in horizontal position, as the casting of the beam in reality. After seven days the samples were rotated for 180 degrees and the second composite slab was casted in horizontal position with same strength class concrete.

Figure 3. Casting of the concrete

2.1 TESTING THE STRENGTH OF THE CONCRETE

After every casting of the concrete a sample was taken for testing the strength of cubes with dimensions 150x150x150mm. the testing of the cubes for the strength of the concrete was carried out on the 29th day from the

casting of every concrete slab. For concrete strength class C25/30, according to EN 1992, the strength of cylinder is f_{ck}=25N/mm2, and the strength of cube is $f_{ck,cube}$=30N/mm2.

Because of the time needed for application of the measuring equipment, the test models were tested on the 34th, 35th and 38th day from the casting of the concrete slab, i.e. 5th, 6th and 9th day from the testing of the concrete samples.

The results of the first casting are with standard deviation of 1.95 and resulted with strength of cube $f_{ck,cube}$=31.71MPa, +5.7% from the specified strength. The second casting is with standard deviation of 0.46 with strength of cube $f_{ck,cube}$=30.19MPa, +0.6% from the specified strength.

2.2 TESTING THE STRENGTH OF THE STEEL

The yield strength, the tensile strength and the maximum elongation of a representative sample of the shear connector material, steel beam, reinforcement and steel sheeting is determined.

The reinforcement steel is class B, in accordance with EN 1992-1-1, Annex C, table C.1 and C.3N, with yield strength of f_{yk}=597MPa, tensile strength f_{uk}=662MPa, with k=f_{uk}/f_{yk}=1.11 and ε_{uk}=9.9%.

The steel for the headed studs is class S235J2+C450, in accordance with EN 13918, with yield strength f_y=502MPa, tensile strength f_u=552MPa, with k=f_u/f_y=1.10 and δ=18.5%.

The steel for the steel sheeting deck is class S550GD Z275, in accordance with EN 10147, with yield strength f_y=675MPa, tensile strength f_u=770MPa, with k=f_u/f_y=1.14 and δ=24.6%.

The steel for the beam is class S275JR, in accordance with EN 1993, with yield strength f_y=275MPa, tensile strength f_u=424MPa, with k=f_u/f_y=1.54 and ε_u=18.9%.

The results from the testing of the steel meet the requirements from EN1992 and EN 1993.

2.3 TESTING PROCESS

The tree samples for the modified testing of the behaviour of the shear connectors are tested in the same environment, with same testing equipment and testing conditions.

The testing is carried out in accordance with EN 1994, Annex B, with cycled loading steps

to 40% and then 25 cycles from 5% to 40%. After the cycled loads, the samples were loaded until failure in time not less than 15 minutes.

For the purpose of the testing, measuring and loading equipment is used. The load us applied through 100 ton press, where the force is regulated with electronic dynamometer. The longitudinal slip between the concrete slab and the steel section is measured with 4 electronic and 4 dial comparators. The accuracy of the testing equipment is in the range of ±1.5%.
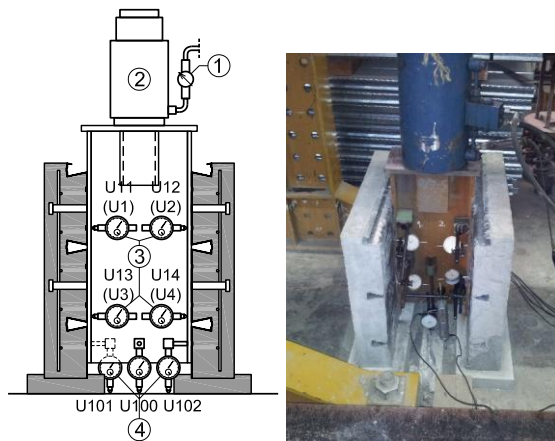

Figure 4. Disposition of the loading and measuring equipment

Where 1) is dynamometer for load measuring, 2) is 100 ton press for load application, 3) dial (U11-U14) and electronic (U1-U4) comparators for transverse separation, 4) electronic comparators (U100-U102) for longitudinal slip.

The electronic equipment is connected to HBM Quantum data acquisition system amplifier with direct connection to computer. The measuring of the electronic equipment is carried out through the whole testing in real time.

2.4 ANALYSIS OF THE DESIGN RESTITANCE AND EXPECTED RESULTS

The analysis of the design resistance of the shear connectors is made in accordance with EN 1994-1-1 (6.6.3.1), for headed stud type Nelson with d=19mm and h_{sc}=100mm. The headed studs are through deck welded to the beam. The steel sheeting is type Bondeck 600 with thickness of t=1.0mm.

The designed resistance of the headed stud, automatically welded through deck in accordance with EN 14555, is determined

according to EN 1994-1-1, (6.18), (6.19) and (6.21).

$$P_{Rd}^{(1)} = \frac{0.8 \cdot f_u \cdot \pi \cdot d^2/4}{\gamma_V} = 90.68 \text{kN} \qquad (2)$$

$$P_{Rd}^{(2)} = \frac{0.29 \cdot \alpha \cdot d^2 \cdot \sqrt{f_{ck} \cdot E_{cm}}}{\gamma_V} = 73.73 \text{kN} \qquad (3)$$

$$\text{Where } \alpha = 1 \text{ for } h_{sc}/d = 5.26 > 4 \qquad (4)$$

$$\min\left(P_{Rd}^{(1)}, P_{Rd}^{(2)}\right) = P_{Rd}^{(2)} = 73.73 \text{kN} \qquad (5)$$

Where,

- f_u is specified ultimate strength of the stud connector,

- f_{ck} is characteristic cylinder compressive strength,

- γ_v is the partial safety factor, recommended value 1.25,

- h_{sc} is the overall height of the stud

- d is the diameter of the stud.

For steel sheeting with ribs transverse to the length of the beam, reduction factor is calculated according to EN 1994-1-1, (6.23)

$$k_t = \frac{0.7}{\sqrt{n_r}} \cdot \frac{b_o}{h_p} \cdot \left(\frac{h_{sc}}{h_p} - 1\right) = 1.47 > 1 \qquad (6)$$
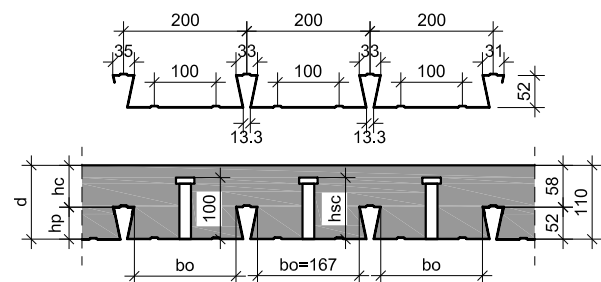
Figure 5. Steel sheeting, headed studs and concrete slab

For value of the reduction factor k_t>1, table 6.2 from EN 1994-1-1 is used, where the upper limit for the reduction factor is $k_{t,max}$=0.70.

$$P_{Rd} = k_t \cdot P_{Rd}^{(2)} = 51.61 \text{kN} \qquad (7)$$

The expected results, without the safety factor γ_v=1.25, for 4 studs per side is:

$$P_{Rd,U} = 2 \cdot 4 \cdot 1.25 \cdot 51.61 = 516.10 \text{kN} \qquad (8)$$

2.3 RESULTS FROM THE TESTING

In Table 1 the results from the testing of the three specimens are given with the measured strength of the force of failure ($P_{Rk,U}$) for eight studs, and the analyzed values of the strength of one headed stud.

Table 1. Results from the testing

$P_{rd,(1)}=f_u/f_{ut}\cdot P_{Rk,(1)}/\gamma_v \leq P_{Rk,(1)}/\gamma_v$			
Specimen	П 1	П 2	П 3
P_{Rd} [kN]	51.61		
$P_{Rd,U}$ [kN]	516.10		
$P_{Rk,U}$ [kN]	602.86	561.82	578.02
P_{Rk} [kN]	542.57	505.64	520.22
$P_{Rk,(1)}$ [kN]	67.82	63.21	65.03
f_u/f_{ut}	0.996		
γ_v	1.25		
$P_{Rd,(1)}$ [kN]	54.04	50.36	51.81
Diff. [%]	+4.71	-2.42	0.39
$P_{Rd,D}$ [kN]	51.84		

Where P_{Rd} is design resistance of one stud including the partial safety factor, $P_{Rd,U}$ is ultimate design resistance of eight studs, without the partial safety factor, $P_{Rk,U}$ is ultimate design resistance of eight studs from the testing, P_{Rk} is reduced ultimate design resistance of eight studs from the testing, according to EN 1994-1-1, B2.5, $P_{Rk}=0.9\cdot P_{Rk,U}$. $P_{Rk,(1)}$ is reduced ultimate design resistance for one stud, $P_{Rd,(1)}$ is design resistance of one stud including the partial safety factor from the testing, $P_{Rd,D}$ is design resistance for the stud from the three specimens, statistical evaluated from all the results in accordance with EN 1990, Annex D.

The difference in negative resistance of -2.42% is great part in the range of the accuracy testing equipment of ±1.5%. The deviation results from the tree specimens is not bigger than 10%, and with the design value of $P_{Rd,D}$=51.84kN>P_{Rd}=51.61kN, can be concluded that the headed studs meet the requirements given in EN 1994.

In Figure 6 (up left and right, down left) P-δ diagrams from the cyclic loading of every specimen is given separately. Additionally, (down right) the determination of the slip capacity δ_u is given, in accordance with EN 1994.
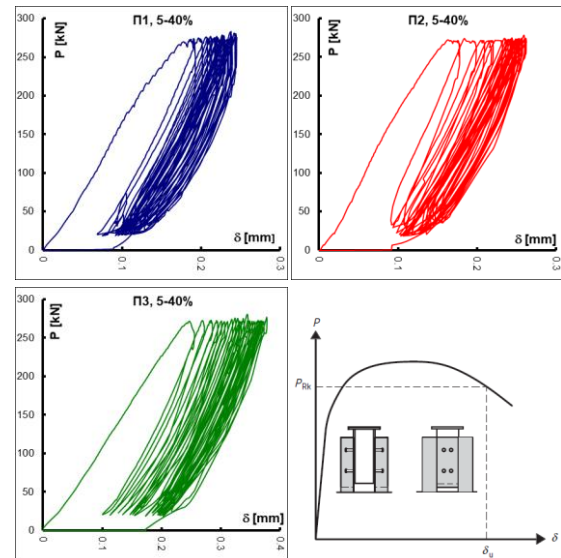
Figure 6. P-δ diagrams and slip capacity

In Figure 7 the determination of the slip capacity from the P-d diagram is given, where $P_{Rk,(1)}=0.9\cdot P_{Rk,U}$ is reduced ultimate design resistance from the testing for one headed stud. From the value of $P_{Rk,(1)}$ and the P-δ diagram from the testing, the value of the slip capacity δ_u can be determined. The diagrams of all specimens are given (down left), including the diagram, with the average diagram (AM) if needed for further analytical research of the behaviour of the shear connectors.
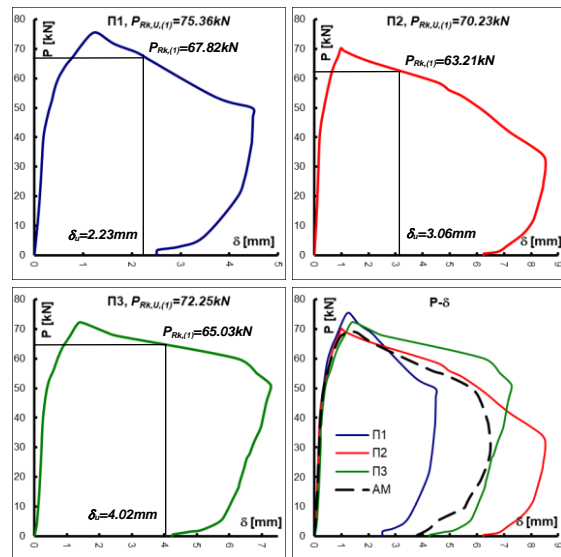
Figure 7. P-δ diagrams, slip capacity determination

The values of the determined slip capacity for each specimen are 2.23mm for П1, 3.06mm for П2 and 4.02mm for П3, where according to EN 1994-1-1, Annex B, the value from all three specimens is:

$$\delta_{uk} = 0.9 \cdot \delta_{u,min} = 2.01 \text{mm} \qquad (8)$$

The value of the slip capacity from all specimens can be also determined with statistical evaluation from the results in accordance with EN 1990, Annex D, in which case the value is δ_{uk}=3.17mm.

There are no significant measured values of transverse separation between the steel beam and the concrete slab.

2. CONCLUSION

The design resistance in dependence of the concrete slab, with all dimensions and concrete strength class, determinates the main resistance of the headed stud shear connectors. If design resistance is needed to be determined not from the concrete slab, but from the headed stud, then lower quality steel for the stud or greater concrete strength class is required.

The value of the slip capacity is δ_{uk}<6mm, which means that the shear connectors from this testing case can be applied for achievement of full plastic capacity of the designed cross section.

For more ductile behaviour of the structure, a smaller diameter or lesser strength quality for the headed stud shear connector is required.

REFERENCES

[1] EN 1994-1-1: Eurocode 4: Design of composite steel and concrete structures – Part 1-1: General rules and rules for buildings, CEN, 12.2004, +AC 04.2009, pp. 55 – 60, 110 – 113.

[2] Popovski D., "Experimental and theoretical research of the effects of composite steel and concrete structures for continuous beams", doctoral dissertation, 2015, Faculty of civil engineering in Skopje, UKIM, pp. 43 – 58.

[3] Popovski D., Cvetanovski P, Partikov M., "Testing the behaviour of shear connectors", MASE 16 international symposium, October 2015, pp. 539 – 548.

[4] Popovski D., Cvetanovski P., Partikov M., "Comparison of continupous composite beams behaviour", Scientific Journal of Civil Engineering, Volume 5, Issue 1, July 2016, pp. 33 – 38.

[5] Cvetanovski P., "Composite structures, printed lectures", 2011, Skopje, R. Macedonia.

[6] Dumovic D., Androic B., Lukasevic I., "Composite structures according to Eurocode 4, Worked Examples", 2014, Ernst & Sohn.

[7] Konrad M., Kuhlmann U., "Headed Studs Used in Trapezoidal Steel Sheeting According to Eurocode 4", SEI, Volume 19, No. 4, 2009.

[8] Galjaard H. C., Walraven J. C., "Static Tests on Various Types of Shear Connectors for Composite Structures", RILEM Publications, SARL, 2001.

D. Popovski, M. Partikov, P. Cvetanovski

AUTHORS

Zlatko Srbinoski
PhD, Full Professor
University "Ss. Cyril and Methodius"
Faculty of Civil Engineering – Skopje
srbinoski@ gf.ukim.edu.mk

Zlatko Bogdanovski
PhD, Assistant Professor
Ss. Cyril and Methodius University
Faculty of Civil Engineering – Skopje
bogdanovski@gf.ukim.edu.mk

LAMBERT NORMAL CONIC PROJECTION WITH TWO STANDARD PARALLELS FOR TERRITORY OF THE REPUBLIC OF MACEDONIA

In this paper basic formulas of Lambert's normal conformal conic projections are given, as well as the results of the basic elements calculation of conformal conic projection with two standard parallels applied on the territory of the Republic of Macedonia.

This is publication in which some advantages of this cartographic projection are shown in terms of Gauss-Kruger projection as an existing state cartographic projection.

Keywords: Lambert's conic projections, conformal projections, line distortions.

1. BASICS OF THE NORMAL CONIC PROJECTIONS

The conic projections in general are mapping of Earths ellipsoid on shape of cone, with previously defined conditions, where the cone can cut or touch the ellipsoid.

Depending on the cone axis position, conic projections can be: normal, oblique and transversal.

In the normal conic projections (which are with biggest application), the Earth is approximated with rotating ellipsoid. Most important thing is layout of the main network (network of meridians and parallels) of conic projections, which is very simple and therefore these projections are widely used.

Namely, the meridians are mapped as straight lines that are intersecting in the top of the cone and represent its generating lines, while the parallels are mapped as circular arcs with given radiuses relative to the center which is located in intersection of the meridians - S (Figure 1). The same layout is normal network (the network of verticals and almucantars) at the transversal conic projections.
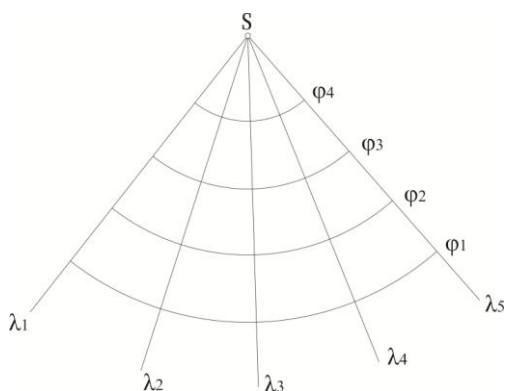
Figure 1. Layout of the main network of normal conic projections

Figure 2. Coordinate systems of the conic projections

The network of meridians and parallels in plane is getting when the cone on which is performing mapping will be cut by one generating line.

The points in conic projections are determining with polar coordinates (δ and ρ) which are shown in next equations:

$$\delta_T = \kappa\lambda \qquad \rho_T = f(\varphi_T) \qquad (1)$$

δ_T - polar angle between starting meridian and meridian through a point,

ρ_T - radius vector, which is radius of the parallel through a point in projection

κ - constant of the projection

f - final, continuous and unambiguous function

λ - difference between longitude of the meridian through a point and longitude of the starting meridian (which is representing the x-axis of the conic projection)

φ_T - latitude of the point.

Besides the polar coordinates, in conic projections are present rectangular coordinates in a plane (y, x). In addition of these, it is common for x-axis to be taken the projection of the central meridian of the mapping zone, which is coinciding with polar axis. The beginning of the coordinate system which is located at the intersection of the meridians or in intersection of the x - axis with some pre-determined parallel (Figure 2).

Connection between polar and rectangular coordinates is given as:

$$y = \rho \sin \delta \qquad (2)$$

$$x = \rho_p - \rho \cos\delta \quad \text{and} \quad x' = \rho \cos\delta$$

ρ_p - radius of the arc of the parallel which is passing through the origin O.

It is already known that the linear scales along the meridian (m) and along the parallel (n) are obtained based on the general equation of the cartographic projections in polar coordinates, from where for normal conic projections it must be taken into account that $\varepsilon = 0$, i.e. sec $\varepsilon = 1$, from where the equations for calculating of linear scales along the meridian and along the parallel are as follows:

$$m = -\frac{d\rho}{M \cdot d\varphi}$$

$$(3)$$

$$n = k\frac{\rho}{r} = \frac{k\rho}{N\cos\varphi}$$

Based on expressions (3) for area scale (p) we can get next equation:

$$p = m \cdot n = -\frac{k\rho \; d\rho}{MN\cos\varphi \; d\varphi} \qquad (4)$$

If we take into account previous equation, the formulas for normal conformal conic projections are:

$$\delta = k\lambda$$

$$\rho = \frac{K}{U^k}$$

$$x = \rho_p - \rho\cos\delta$$

$$y = \rho\sin\delta \qquad (5)$$

$$m = n = k\frac{\rho}{r} = \frac{k}{r}\frac{K}{U^k}$$

$$p = m^2 = \left(\frac{k}{r}\frac{K}{U^k}\right)^2$$

$$\omega = 0$$

Z. Srbinoski, Z. Bogdanovski

2. LAMBERT NORMAL CONFORMAL CONIC PROJECTION WITH TWO STANDARD PARALLELS

German scientist Lambert (Johann Heinrich Lambert) is the originator of the conformal conic projections, in whose paper *"Beiträgezum Gebrauche der Mathematik und deren Anwendung"* (Contributions to the usage of mathematics and its application), published in Berlin in 1772, for the first time these projections are mathematically defined. According to his achievements, these projections are called Lambert conformal conic projections.

Five types of conformal conic projections with one or two standard parallels are commonly encountered in practice. The so called fifth variant or normal conformal conic projection with two standard parallels applied over territory of the Republic of Macedonia will be presented in frame of this paper. This projection is mostly used for preparation of large scale maps, and for that in the past was and in many countries already is state cartographic projection.
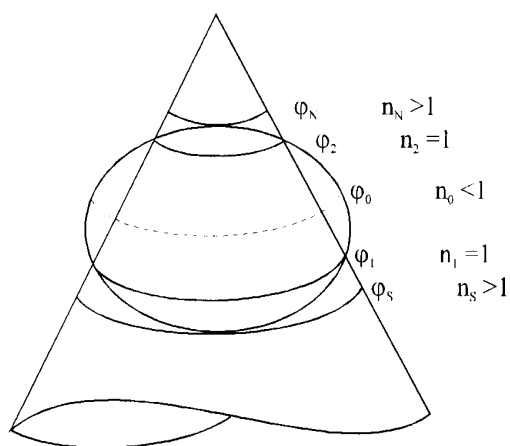

Figure 3. Change of the scale in conformal conic projections

It is about projection of the Earth's ellipsoid on cutting cone, which cuts the ellipsoid in two standard parallels where there is no linear distortions ($n_1 = n_2 = 1$).

The standard parallels and parameters of the projection (k, K) are determining in relation with next conditions:

- The scales of the last parallels for defined territory to be mutually equal

$$n_S = n_N$$

- Largest scale to be more than one as smallest scale is smaller than one

$$n_S - 1 = 1 - n_o$$

With stated conditions are obtained minimal values and most favorable schedule of linear distortions for territory of projecting.

Starting from the first condition ($n_S = n_N$), the value of constant of the projection (k) is calculating with:

$$k = \frac{\log r_S - \log r_N}{\log U_N - \log U_S} \qquad (6)$$

Through known value of constant of the projection (k) next step is to determine the value of the latitude on parallel with minimal value of linear scale:

$$\varphi_o = \arcsin (k) \qquad (7)$$

The constant of the integration (K) shall be determined with second condition which is shown with next equations:

$$n_S = 1 + \varepsilon \qquad n_N = 1 + \varepsilon \qquad n_o = 1 - \varepsilon \quad (8)$$

ε - Absolute value of difference between maximal and minimal value of the scale and one

Considering of the constant of the linear scale along the meridian and along the parallel and after series of mathematical transformations, it's getting the value of the constant of the integration which is defined with next formula:

$$K = \frac{2r_S U_S^k r_o U_o^k}{k\left(r_S U_S^k + r_o U_o^k\right)} = \frac{2r_N U_N^k r_o U_o^k}{k\left(r_N U_N^k + r_o U_o^k\right)} \qquad (9)$$

The other equations that define the Lambert normal conformal conic projection with two standard parallels are identical to the equations of expression (5).

3. LINEAR DISTORTIONS AT CONFORMAL CONIC PROJECTION WITH TWO STANDARD PARALLELS

In process of choosing a state map projections is not crucial the absolute amount of distortions, but their favorable layout. If it is made analyses of formulas (basic equations), can be concluded that the linear distortions and areas at normal conformal conic

projections are functions only of latitude (φ), respectively:

$$m = n = f(\varphi)$$

This implies that the distortion isograms at these projections are coinciding with parallels.

In Lambert normal conformal conic projection with two standard parallels, the cone which is for projecting cuts the ellipsoid in two parallels which are called the **standard parallels.** As we emphasized, the linear scales of distortions at these parallels are equal to 1 ($n_1 = n_2 = 1$) and therefore, among them there are no linear distortions.

In the area between standard parallels the value of linear scale is smaller than one ($n < 1$) and the linear distortions are with negative value. In this area projections of parallels are with smaller length than the same parallels on the ellipsoid. The minimal value of the linear scale of the distortions achieves the parallel with latitude φ_o, which determining is depending from conditions of the projection.

The distortions of lengths rapidly growing on north and south from standard parallels and its maximum values are reaching at boundary parallels on the mapping area. The value of linear scale is bigger than one ($n > 1$) from where the distortions of lengths are with positive value.

In figure 4 is presented schematic overview for distribution of the distortions in conic projections with two standard parallels.
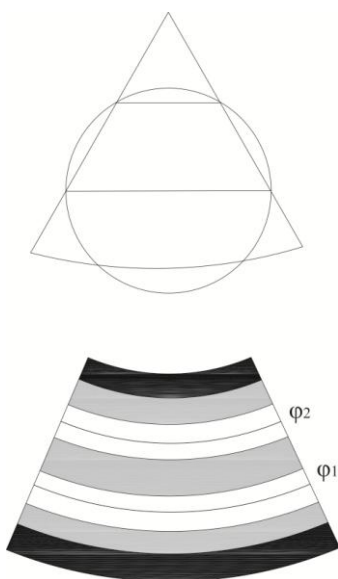

Figure 4. Distribution of distortions of conic projections with two standard parallels (darker areas indicate larger distortions)

4. ELEMENTS FOR DEFINING OF LAMBERT NORMAL CONFORMAL CONIC PROJECTION WITH TWO STANDARD PARALLELS FOR THE TERRITORY OF THE REPUBLIC OF MACEDONIA

For application of this map projection for territory of the Republic of Macedonia, is necessary to determine northern and southern points of the territory. Their coordinates were read from TM 25 and they are:

point (name)	geographic coordinates	
	φ	λ
northern *Aniste*	42° 22' 20"	22° 18' 05"
southern *Markova noga*	40° 51' 14"	21° 07' 48"

With usage of the presented values (where φ_S is rounded to 40° 51' 15") and application of the aforementioned conditions were obtained parameters for normal conformal conic map projection with two standard parallels for the territory of the Republic of Macedonia. Thereby, the standard parallels are with values:

$\varphi_1 = 41^o$ 04' 38"   and $\varphi_2 = 42^o$ 09' 02"

These are parallels where the cone is cutting the ellipsoid and linear distortions are equal to 0. The parallel in which are maximal distortions with negative sign (φ_o) is with value 41° 36' 49".

The maximal value of the linear distortions is +4.4 cm/km at parallels (φ_S and φ_N) and analogous to that, based on the second condition, the value -4.4 cm/km is at parallel φ_o which is passing approximately through the center of the R. of Macedonia.
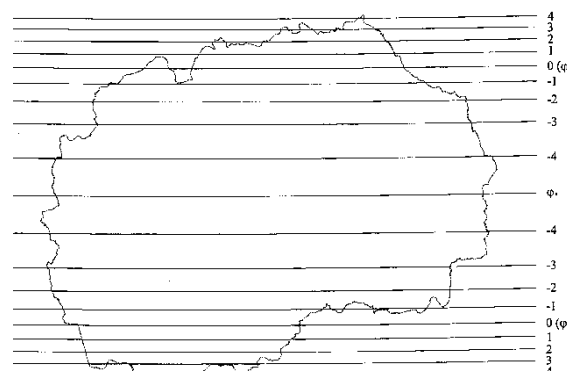

Figure 5. Distribution of the distortion isograms at Lambert conformal conic projection for R. of Macedonia

Z. Srbinoski, Z. Bogdanovski

The coordinate system of rectangular coordinates in mapping plane can be set arbitrarily, but in this publication the authors according to their research decide x-axis to be the meridian with longitude $\lambda = 21° \, 45'$, and for y-axis is adopted the intersection of the x-axis with parallel $41° \, 35'$. On a coordinate origin obtained in that way, 500000 m are added on both axes, with aim to eliminate the negative coordinates (figure 6).
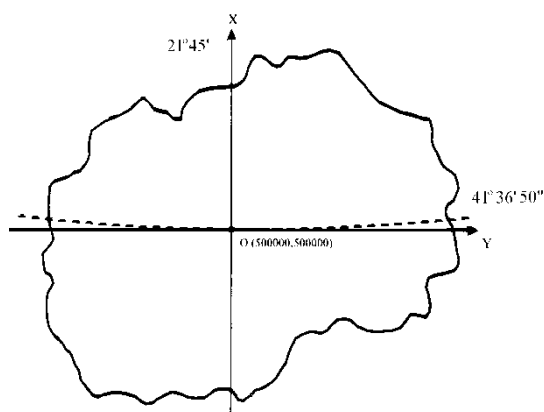

Figure 6. Coordinate system of Lambert conformal conic projection for R. of Macedonia

The positive properties of the Lambert conformal conic projection with two standard parallels can be summarised in the next conclusions:

- The linear distortions of the lengths for all territory of the R. of Macedonia are in range from +4.4 cm/km till -4.4 cm/km.

- The distortions of lengths are 70% smaller than the distortions in actual Gaus-Kruger projection.

- The shape of the territory of the R. of Macedonia is suitable for use of conic projections, because of its elongation along parallels. Namely "width" of the territory of the R. of Macedonia expressed by distance between endings meridians at central longitude is approximately 216 km, while the "length" expressed by distance between endings parallels is approximately 168.5 km.

- Correct distribution of the distortions where distortion isograms represent parallels with known latitude.

- Correct layout of main network where meridians are straight lines and parallels are circular arcs with given radius. The correct layout of the main

network enables easy calculations of some important parameters such as convergence of the meridian in known point of the projection.

- Relatively simple mathematical calculations which are seriously worked out in countries where this projection is used as state projection.

- There are no angle distortions.

REFERENCES

[1] Borčić B. (1955): *Matematička kartografija (kartografske projekcije)*, Tehnička knjiga, Zagreb;

[2] Jovanović V. (1983): *Matematička kartografija,* Vojnogeografski institut, Beograd.

[3] Rajaković M. Lapaine M. (2010): *The best conic conformal map projection for the territory of Croatia*, Cartography and Geoinformation, Vol. 9, No 14.

[4] Рибароски Р., Пауновски Б., Марковски Б., Јованов Ј., Србиноски З. (1998): *Избор на најпогодна картографска проекција за претставување на територијата на Р. Македонија*, Научна тема, УКИМ, Скопје.

[5] Србиноски З. (2001): *Прилог кон истражувањата за дефинирање на нова државна картографска проекција*, Докторска дисертација, Градежен факултет, Скопје.

[6] Србиноски З. (2012): *Математичка картографија*, универзитетски учебник, Градежен факултет, Скопје.

Имаіте доверба во Кнауф.
Чувствуваіте се заштитен.

Кога ќе избие пожар, секоіа секунда е драгоцена. Затоа препуштете іа Вашата доверба во новата програма противпожарни производи од европскиот водечки бренд за производство на градежни материіали: Knauf FireWin. Зголемете іа безбедноста на луѓето и обіектот.

- Противпожарни плочи
- Противпожарен малтер за внатрешна употреба
- Противпожарен малтер за надворешна употреба
- Противпожарна боіа
- Противпожарни манжетни

EFFECTS OF WASTE GLASS ON PROPERTIES OF HARDENED CONCRETE

Authors

Todorka Samardzioska

PhD, Full Professor
University Ss. Cyril and Methodius
Faculty of Civil Engineering – Skopje
samardzioska@gf.ukim.edu.mk

Jasna Grujoska

MSc, Younger Assistant
FON University - Skopje
Faculty of Architecture
jasna.grujoska@fon.edu.mk

Vesna Grujoska

MSc, Associate Degree
University Ss. Cyril and Methodius
Faculty of Civil Engineering – Skopje
vesna.grujoska@gf.ukim.edu.mk

Darko Moslavac

PhD, Full Professor
University Ss. Cyril and Methodius
Faculty of Civil Engineering – Skopje
moslavac@gf.ukim.edu.mk

Katerina Donevska

PhD, Full Professor
University Ss. Cyril and Methodius
Faculty of Civil Engineering – Skopje
donevska@gf.ukim.edu.mk

Use of renewable materials instead of natural resources is one of the best approaches in sustainability of the concrete industry. Glass, being non-biodegradable, is not suitable for addition to landfill. On the other hand, 18% of the total waste in Macedonia is waste glass.

This paper is a part of a bigger research project, which has been undertaken at the Faculty of Civil Engineering in Skopje, to develop new applications for waste glass as an aggregate for concrete. More precisely, the aim was to investigate the feasibility of utilizing recycled glass as a concrete aggregate in fine aggregates and fine glass powders. Four different mixtures have been made: the glass is used as partial (50%) or entire replacement (100%) of the fine aggregate (0-4mm) in concrete, with and without admixtures. Couples of samples were prepared for each recipe and properties of fresh concrete and hardened concrete were tested at 3, 7, and 28 days.

Both, properties of fresh and hardened concrete were tested. This paper presents mainly the latter properties: different strengths of the concrete with various percentage of waste glass as a fine aggregate.

Results from the laboratory experiments show that the concrete containing waste glass has almost identical or even better properties as the standard concrete, as well as great economical and ecological savings. Results demonstrate that the use of waste glass as aggregate facilitates the development of concrete towards a high structural level.

Concrete using waste glass can be commercially wide used for specific products such as paving stones, curbs, concrete masonry blocks, terrazzo tiles and precast façade panels.

Keywords: concrete, waste glass, waste management, properties of concrete, sustainable development

1. INTRODUCTION

Concrete is one of the most used and most important building materials and necessity of it increases daily with the increased development of the civil engineering. The environmental and economic concerns are the biggest challenge that concrete industry is facing nowadays. Huge amounts of concrete that are produced require large amounts of aggregate. Aggregate used for concrete production is mostly of natural origin (sand, gravel, crushed stones, etc.). However, the continued exploitation of these natural resources, which are non-renewable, leads to destruction of the nature.

For these reasons, many countries restrict or completely prohibit the exploitation of natural aggregate for concrete and they are oriented towards finding new alternatives for obtaining artificial aggregates. Processing and application of certain waste materials as substitutes for natural aggregate is one of the best ways to make the concrete industry sustainable. With this procedure, the problem of excessive waste is solved on one hand, while on the other hand the possibilities for recycling are increased. One of the materials that are suitable for such processing is glass.

Huge amounts of waste glass are created every day. Although it is known that glass is not naturally degradable material, the biggest part of the waste glass ends up in landfills. In most European countries, the total amount of waste glass can be recycled only about 20% in the glass industry. However, Japan has a glass recycling rate of about 90%. Because of its structure, the glass can be recycled many times without losing its properties. Recycling only applies to glass containers (bottles and jars) that satisfy specific criteria of purity. On the other hand, windows, mirrors, glasses, TV, monitors, lamps etc are mainly not recycled.

In Macedonia, the entire glass waste from different sources (around 18 % of the total waste according to the Strategy for Waste in Republic of Macedonia) is deposited or exported. It is very important to find a solution to this waste, both in terms of preserving the environment and in terms of solving the problem of excessive waste. The processing of waste glass and its use as aggregate for concrete provides major economic and environmental savings: prevents the exploitation of natural resources, saves energy, reduces the amount of waste material, reduces the price of concrete etc.

Few disadvantages due to the using recycled glass exist, as well. They relate to impurities that may occur in the raw material, the price for purchase of scrap glass, the quality of the new material etc. Nevertheless, due to the fact that the glass is one of the few materials in the nature which can be endlessly recycled, the purpose of this paper is to demonstrate a sustainable development of the industry for recycling glass and natural impacts on the Macedonian economy.

Research with laboratory experiments was conducted to further explore the use of waste glass as fine aggregates for concrete. The most important physical and mechanical properties of the concrete made with variable quantity of processed waste glass aggregates and possibilities of its application are presented in the paper. The density, porosity, compressive strength, tensile strength, flexural strength, water absorption of the concrete with different percentage of glass aggregate have been tested.

2. STATE OF THE ART

Many researchers around the world have performed aggregate replacement studies using waste glass. The general aim was to define a quantity of glass that will provide optimal strength properties of the concrete.

The influence of the waste glass on the mechanical properties of concrete has been researched by many researchers, including Du and Tan (2014), [1], Multon et al. (2008), [2], Newes and Zsuzsanna (2006), [3], Xie and Xiang (2003), [4], Johnson (1974), [5]. Their results show that the aggregate of waste glass decreases the concrete strength, in general. They attribute this behaviour to a strong chemical reaction between the quartz from the glass and the alkalis in the cement paste, which can lead to expansion and cracking of concrete.

Recently, there have been experimental investigations of Rubaie and Fouad, [6], which evaluate the properties of the concrete mixture containing waste glass up to 20% of the sand volume. The results show that the concrete mixture containing waste glass shows a very slight decrease in the compressive strength and tensile strength compared to reference classic mixtures.

Ling and Poon, [7], have been investigating the alkali-silica reaction in concrete with waste glass and the influence on the properties of

T. Samardzioska, J. Grujoska, V. Grujoska, D. Moslavac, K. Donevska

fresh and hardened concrete, as well as on decorative concrete in civil engineering and architecture.

Following results were obtained in a survey conducted by Malik et al, [8]: 20% replacement of fine aggregate indicates increased compressive strength for 15% at 7 days and 25% increased strength for 28 days. The fine aggregate can be replaced with glass up to 30% of its weight, with the compressive strength at 28 days increased by 9.8% compared to standard concrete.

Gautam et al., [9], found that waste glass can effectively be used as fine aggregate replacement, but the optimum replacement level of waste glass as fine aggregate is 10%. Marginal decrease in the compressive strength is observed at 30 to 40% replacement level of waste glass with fine aggregate.

Furthermore, Meyer et al., [10], found that concrete made with recycled glass aggregate is highly durable with great thermal insulation and moisture protection. These properties are inherited from the glass itself.

Therefore, different studies show various results and conclusions on the use of waste glass as fine aggregate in the concrete. However, almost none of them suggest replacement of the fine aggregate with glass for more than 30%.

3. LABORATORY TESTING

This study shows the opportunities for using waste glass in concrete industry. Performed work, presented in this paper, is a part of a larger on-going project, which examines the influence of different types of waste glass as an aggregate in concrete on the concrete's properties. The front glass from CRT monitors is used for this purpose. The glass is used as partial (50%) or entire replacement (100%) for the fine aggregate (0-4mm) in concrete. Four recipes have been made:
- normal concrete (0% glass),
- concrete containing 50% waste glass as fine aggregate,
- concrete containing 100% waste glass as fine aggregate, and
- concrete with admixtures (air entrainers and super-plasticizers) containing 50% waste glass as fine aggregate.

The mixtures have water to cement ratio of 0,45. Couple of samples were prepared of

each recipe and the properties of fresh concrete and hardened concrete.

Figure 1. Glass and natural stone aggregate

The following samples were made out of each recipe for concrete mixture:
- 9 cubes (15/15/15 cm) for testing of compressive strength
- 3 cylinders (15/30 cm) for testing of slitting tensile strength (Brazilian test)
- 3 prisms (10/10/50 cm) for testing of flexural strength
- 6 cubes (15/15/15 cm) for testing waterproofing.

Porosity, density and consistency of the fresh concrete were measured for all recipes. Afterwards, the cube moulds were fixed and oiled, i.e. prepared for filling with fresh concrete. The fulfilment of the molds was carried out by compacting with vibration, ensuring the shape of the samples, Fig. 2. De-moulding of the samples was carried out after 24 hours, after the hardening of the concrete, with utmost care to prevent any damage to the samples. The samples were stored in standardized laboratory conditions, and tested at 3, 7 and 28 days.

Figure 2. Preparing of concrete samples

4. ANALYSIS OF RESULTS

4.1 COMPRESSIVE STRENGTH

The compressive strength was tested on cube samples with dimensions 15/15/15 cm. They were tested in testing machine – press, ac-

cording to the standard EN 12390-4, Fig. 3. The specimens were set centrally to the lower plate of the press; therefore the applied load is in direction normal to the sample. The load has been applied gradually with constant step of 10%, until a greater load was achieved than the range selected for application.

Figure 3. Press for testing compressive strength

The compressive strength was tested in series of three cubes each, at 3, 7, 28 days, as it is presented at Figure 4.

By increasing the proportion of glass in the concrete, mechanical properties of the concrete at 7 days were improved, Figure 5.

Figure 4. Tested cubes of recipe 2 for compressive strength at 28 days

Values of the compressive strength of the concrete with 50% and 100% glass as fine aggregate are greater than the ones of the standard concrete. The best compressive strength exhibits the concrete with 100% glass in the first fraction (f_c = 39,7 MPa). In comparison to the strength of standard concrete (f_c = 35,1 MPa), the increase in the strength is 13%.

Similar results appear for testing at 28 days, Fig. 6. The compressive strength for the con-

crete with 50% glass as a fine aggregate is f_c = 46,4 MPa, while for the concrete with 100% glass is f_c = 46,8MPa. Standard concrete in this case showed compressive strength of 44 MPa. Replacement of 50% of the fine aggregate with waste glass shows 5% increase in the compressive strength, while replacement of 100% of the fine aggregate with glass aggregate shows 6% increase in the compressive strength comparing to the standard concrete. Best results were obtained for the fourth recipe (50% glass with admixtures), where the increase in the compressive strength is 12% compared to the standard concrete, see Figure 6.
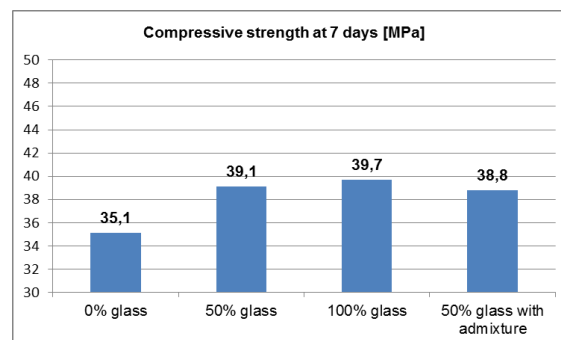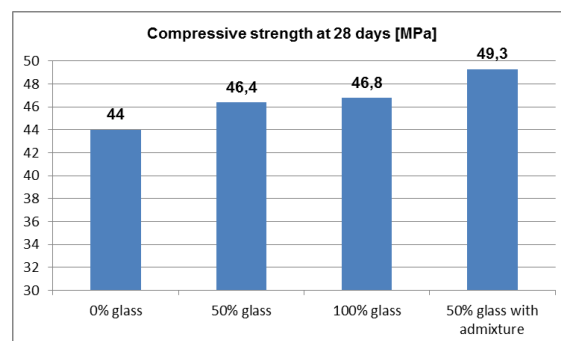

Figure 5. Compressive strength at 7 days

Figure 6. Compressive strength at 28 days

Using glass as a substitute for the fine aggregate, higher values of the compressive strength are obtained, both at an early stage and later stage of hardened concrete. Best values for the compressive strength are obtained at full replacement of the fine aggregate with glass. The range between companion samples from the same set and tested at age of 7 days is from 0,2% to 2,8% of the average strength. Error margins for the companion samples tested at age of 28 days range from 0,8% to 3,6% of the average strength.

4.2 SPLITTING TENSILE STRENGTH

The testing of tensile strength was performed according to the standard MKS EN 12390-6. Tested samples were cylinders with dimen-

T. Samardzioska, J. Grujoska, V. Grujoska, D. Moslavac, K. Donevska

sions 15/30 cm. The testing of the samples was carried out in an appropriate machine (press) according to MKS EN 12390-4, according to the so-called Brazilian method, Fig. 7. During the test, the samples are set centrally in the machine, and load was applied while the upper and lower rollers were placed parallel to each other. The load was applied gradually with step of 10%, until a fracture of the sample under the indicated maximum load.

Figure 7. Brazilian method - testing of specimen with splitting test

In general, tensile strength of the concrete is much lower than its compressive stress. For usual concretes, the ratio between them is 1:10. Testing of the tensile strength with splitting is performed at age of 28 days on three cylindrical samples. Fractured samples are presented in Fig. 8.

Figure 8. Tested specimens – Brazilian method

The concrete of the recipe 2 (with 50% glass), shows best values for the splitting tensile strength, f_{zc} = 3,54 MPa. With increasing the proportion of glass (above 50%), the tensile strengths decrease. Therefore, the concrete recipe 3 (100% of glass for the first fraction) has the weakest splitting tensile strength f_{zc} = 2,90 MPa, as it can be seen in Figure 9.
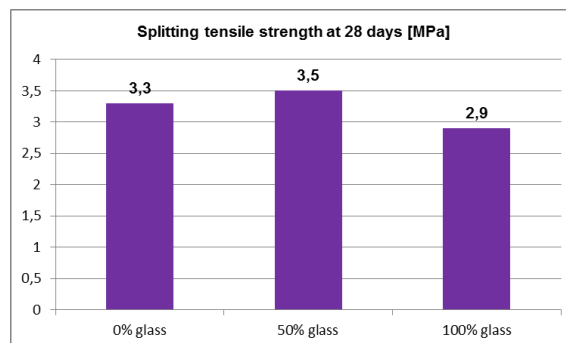

Figure 9. Diagram of splitting tensile strengths at 28 days

The results lead to conclusion that the difference in the values of tensile strengths for various concrete recipes is low. Reason for such a small difference is that the splitting tensile strength of the concrete depends on the relationship between cement stone and grains of the coarse aggregate, rather than on the properties of the fine aggregates.

4.3 FLEXURAL STRENGTH

The flexural strength is not often used for field control and the engineers generally find the use of compressive strength convenient and reliable to judge the quality of the concrete as delivered. However, the designers of pavements use a design theory based on flexural strength. The results of this test method may be used to determine compliance with specifications or as a basis for mixture proportioning, evaluating uniformity of the mixture, and checking placement operations by using sawed beams. It is used primarily in testing concrete for the construction of pavements and slabs.

This test method is used to determine the flexural strength on prismatic specimens with dimensions 10x10x40 cm и 10x10x50 cm, prepared and cured in accordance with the standard MKS EN 12390-4. The testing device comprises: a load roller (which can be rotated and bends) and supporting rollers that can be rotated and pivoted, Fig. 10. Rollers are made of steel with a circular cross-sectional diameter of 10 to 20 mm. Rollers are placed in a way that they can freely rotate around their axes. The test is actually a simulation of a simple beam loaded with a concentrated force in the middle, as it is shown in Fig. 10.

Figure 10. Prisms tested to bending

Samples fractured under flexural stresses are presented in Fig. 11.

Figure 11. Tested specimens for flexural strength

4.4 WATERTIGHTNESS

Determination of the depth of penetration of water under pressure in hardened concrete was performed according to the standard MKS EN 12390-8. Concrete cubes with dimensions of 15/15/15 cm were testing samples. The samples were water cured, and water is applied under pressure of 500 ± 50 kPa for 72 hours to the previously roughed surface of hardened concrete. The specimens are then split into half, vertically on the side where the water pressure was applied and left to lie on the side that had been exposed to water pressure, as presented in Fig. 12. The maximum depth of penetration of the waterfront is measured.
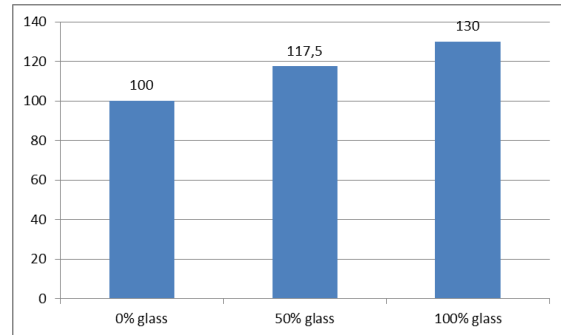

Figure 12. Wet concrete cubes

Figure 13. Average values of water penetration in samples (mm)

From the results presented, it can be noticed that the penetration of water is increased by increasing the percentage of waste glass in concrete, see Figure 13. The highest water penetration occurs in concrete of recipe 3 (100% glass in the smallest fraction).
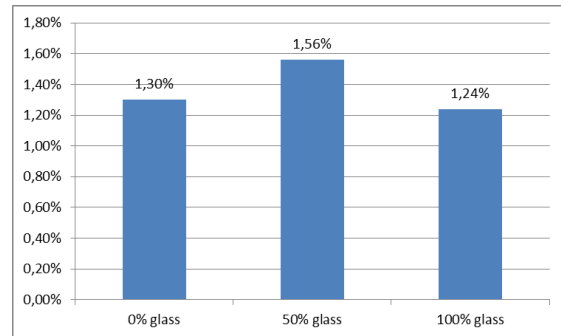

Figure 14. Average values of water absorption, in percentages

Figure 14 shows that the water absorption has the highest value in concrete containing 50% glass from the first fraction. By increasing the amount of glass in concrete (over 50%), the percentage of absorbed water is reduced. Thus, for concrete containing 100% glass, the percentage of water absorption is the lowest and it is 1.24%. This value is also lower in relation to the value for the standard concrete.

5. SUMMARY AND CONCLUSIONS

The research in this paper contributes to new opportunities for using waste glass. An experimental laboratory study of concrete containing a partial or total replacement of the fine aggregate with glass has been conducted. Results on the properties of hardened concrete are analyzed. A comparison of samples of concrete containing glass with samples of standard concrete has been made. The results of these laboratory tests are compared with previous similar experiences in the world.

T. Samardzioska, J. Grujoska, V. Grujoska, D. Moslavac, K. Donevska

The compressive strength increases in concrete with used waste glass instead of gravel aggregate. Both mixtures made with 50% replacement of the fine aggregate with waste glass and with 100% replacement showed improved compressive strengths (up to 12%) in comparison to the standard concrete. As for the tensile strength due to splitting and bending, concrete containing waste glass has almost identical properties as the standard concrete. Regarding the concrete behaviour under water conditions, the percentage of water absorption for the concrete containing 100% glass is the lowest and it is 1.24%.

The idea in this research is to show that the proper use of waste materials can produce a concrete with same or even better properties than the standard concrete and great economic and ecological savings. The recommendations in the world literature for this type of concrete are that it can be used for making non-structural members, mostly for paving large surfaces, curbs, pavements, etc., but not for structural bearing members in structures. However, according to the properties obtained in this experimental study, this type of concrete possesses the same properties as the concrete used for the manufacture of bearing structural members. The concrete containing waste glass as fine aggregate satisfies the requirements for achieving compressive strength of 30 Mpa at age of 28 days, which corresponds to the widely used type of concrete for most of the structural members in buildings. Validation of the physical and mechanical properties of concrete which contains variable amounts of waste glass as an aggregate enables the use of this material for production of environmental material with sustainable significance. This approach solves the problem of excessive waste, contributing to greener and safer environment.

Having opened new opportunities and horizons for application of concrete with aggregate of waste glass, new fields are opened for their further study as well. Use of waste glass as coarse aggregate in concrete presents a potential for new studies. Such a concrete with visible larger fractions of glass in different colours would have a wider use as a decorative material in the civil engineering and architecture. An interesting phenomenon in this material is an alkali - silica reaction that develops over time and its impact on the properties of fresh and hardened concrete. Further tests on concrete with glass waste should be carried out for this purpose, in long periods of time that will allow development of such reaction.

REFERENCES

[1] Du, H. & Tan, K. H.: Concrete with Recycled Glass as Fine Aggregates, Materials Journal, Vol. 111 (2014), No. 1, pp. 47-58.

[2] Multon, S.; Barin, X.; Godart, B. & Toutlemende, F.: Estimation of The Residual Expansion of Concrete Affected by Alkali Silica Reaction, Journal of Materials in Civil Engineering, Vol.20 (2008), No.1, 2008, pp. 54-62.

[3] Newes R. & Zsuzsanna: Strength of light weight glass aggregate concrete, Journal of Materials in Civil Engineering, Vol. 18 (2006), No. 5, pp. 710-714.

[4] Xie Z.; Xiang W. & Xi, Y.: ASR Potentials of glass aggregate in water glass activated fly ash and Portland cement mortar, Journal of Materials in Civil Engineering, Vol. 15 (2003), No. 1.

[5] Johnson, C. D.: Waste glass as coarse aggregate for concrete, Journal of testing and evaluation, Vol. 2 (1974), pp. 344-350.

[6] Rubaie, A. & Fouad, M.: Properties of concrete building units containing crushed waste glass, M.Sc. Thesis, The University of technology, 2007.

[7] Ling, T.C.& Poon, C.S.: Utilization of recycled glass derived from cathode ray tube glass as fine aggregate in cement mortar, Journal of Hazardous materials, Vol. 192 (2011), No.1, pp.451-456.

[8] Malik, M. et al.: Study of concrete involving use of waste glass as partial replacement of fine aggregates, IOSR Journal of Engineering, Vol. 3 (2013), No. 7, pp. 8-13, ISSN: 2278-8719.

[9] Gautam, S.P.; Srivastava, V. & Agarwal, V.C.: Use of glass wastes as fine aggregate in Concrete, J. Acad. Indus. Res., Vol. 1 (2012), No. 6, ISSN: 2278-5213.

[10] Meyer, C.; Egosi, N. & Andela, C.: Concrete with waste glass as aggregate, in "Recycling and Re-use of Glass Cullet", Dhir, Dyer and Limbachiya, editors, Proc. of the International Symposium CTU of ASCE & University of Dundee, March 20, 2001.
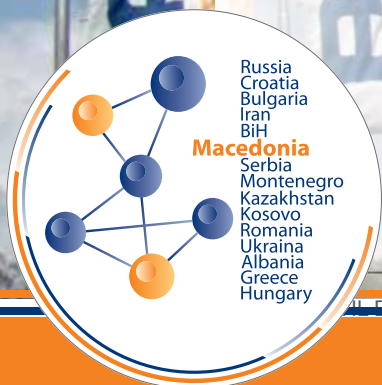
AUTHORS

Aydin Demir

Research Assistant

Faculty of Engineering

Department of Civil Engineering

Sakarya University

Sakarya, Turkey

Hakan Ozturk

PhD, Assistant Prof.

Faculty of Engineering

Department of Civil Engineering

Sakarya University

Sakarya, Turkey

Aleksandra Bogdanovic

PhD, Assistant Prof.

Ss. Cyril and Methodius University

Institute of Earthquake Engineering

and Engineering Seismology IZIIS-Skopje

saska@pluto.iziis.ukim.edu.mk

Marta Stojmanovska

PhD, Assistant Prof.

Ss. Cyril and Methodius University

Institute of Earthquake Engineering

and Engineering Seismology IZIIS-Skopje

marta@pluto.iziis.ukim.edu.mk

Kemal Edip

PhD, Assistant Prof.

Ss. Cyril and Methodius University

Institute of Earthquake Engineering

and Engineering Seismology IZIIS-Skopje

kemal@pluto.iziis.ukim.edu.mk

SENSITIVITY OF DILATION ANGLE IN NUMERICAL SIMULATION OF REINFORCED CONCRETE DEEP BEAMS

In this paper, a parametric nonlinear finite element (FE) study is conducted in order to investigate sensitivity of dilation angle on numerical simulation of reinforced concrete (RC) deep beams. A numerical verification of an existing experimental study of a deep beam is performed via ABAQUS software with different varied values of dilation angle. Results of the experimental and numerical studies are compared in terms of load-displacement behaviors. Results from the analysis show that in conjunction with increase in its value, not only significant increase in ultimate load capacity is experienced, but also more ductile behavior is achieved for RC deep beams.

Keywords: Dilation angle, concrete damage plasticity, finite element analysis, ABAQUS, reinforced concrete deep beam

1. INTRODUCTION

It is a fact that behavior of a structure depends on behavior of its members such as beams, columns, shear walls etc. Therefore, investigation of nonlinear behavior of reinforced concrete (RC) members under static and dynamic loads is very crucial to design safe structures [1]. Moreover it is known that the most reliable and accurate technique to investigate nonlinear behavior of an RC member is to perform an experimental study. However in terms of inconveniency, time, labor and budget, experimental studies have some disadvantages.

Additionally, there are many studies proposing that finite element (FE) analysis comprising an appropriate numerical modeling technique and accurate constitutive material models is a quite reliable and robust alternative tool of experimental studies to investigate nonlinear behavior of RC members [2]. Because of that reasons, FE analysis is widely preferred by researchers.

In order to make a numerical simulation, first a FE model should be verified sufficiently with experimental test results and later on a parametric study should be performed computa-

tionally by numerical analysis. During a numerical verification of a test result to create a FE model, a lot of parameters should be defined and calibrated into the model, e.g., constitutive material models, part (member) sections, mesh and assembly properties etc.

Concrete is a brittle material and experiences volumetric change beyond its elastic limit stemming from cracking and slip along cracked surfaces. The change in volume in brittle materials is generally called as "dilation". Because of the fact that confinement pressure of an RC member is severely affected by the dilation characteristic of concrete, it plays very important role on stress–strain behavior of concrete in compression. A stiffer stress–strain relation can be observed due to increase in the dilation leading to more confinement [3].

Two different constitutive material models for concrete are proposed in ABAQUS/Standard which is an implicit analysis program for analysis of concrete at low confining pressures. They are smeared crack concrete model and concrete damaged plasticity (CDP) model. Additionally, CDP model is relied on the assumption of isotropic damage and takes into account the degradation of the elastic stiffness induced by plastic straining both in compression and tension [4]. In order to create an accurate numerical FE model for an RC member; flow potential, yield surface and some important material parameters such as dilation angle have to be defined to constitute CDP material model.

Mercan et al. [5] conducted a finite element study on numerical modeling of pre-stressed concrete spandrel beams. One of the various parameters investigated in the study for sensitivity of the spandrel beam response is dilation angle (ψ). Analysis results deduce that ψ has a major effect on lateral and vertical deformations at the mid-span of the spandrel beams. While dilation angle has no impact in the elastic regime, the decrease of dilation angle reduces the stiffness of the cracked beam. A dilation angle of 55° was proposed to describe the behavior of confined concrete in the spandrel beam since both reinforcement and pre-stressing provide confinement for the concrete.

In the study of Szczecina and Winnicki [6], some important aspects concerning material constants of concrete i.e. dilation angle, fracture energy etc. and stages of numerical modeling of RC structures were presented. Anal-

yses were performed in ABAQUS software using concrete damage plasticity model of concrete. The study was concluded that a proper choice of dilation angle is very important during modeling of an RC structure behavior using CDP model.

Additionally, Sumer and Aktas [7] proposed some numerical modeling strategies for CDP model in ABAQUS software. Those strategies were developed by checking the model sensitivity against mesh density, dilation angle and fracture energy of concrete. FE models were verified in acceptable range by using results of three different experimental RC beam tests. Analysis results showed that the numerical results are not varying dramatically as the dilation angle changes.

Deep beams are defined in ACI 318-14 [8] code as RC members having a clear span not exceeding four times the overall member depth. They are also loaded on one face and supported on the opposite face. Any default value is not proposed in ABAQUS manuals for dilation angle of concrete and there is no consensus for a constant value in literature for RC deep beams. Because of this reason, the motivation of the study is to investigate the effect of dilation angle on behavior of RC deep beams. For this objective, a numerical verification of an existing experimental study of a deep beam is conducted by utilizing commercial finite element software that is ABAQUS/Standard. Results of the experimental and numerical studies are compared in terms of load-displacement behavior.

2. DILATION ANGLE (ψ)

The concrete damaged plasticity model assumes non associated potential plastic flow implying that the material stiffness matrix is asymmetric; therefore, the unsymmetrical matrix storage and solution implementation should be employed in ABAQUS software. The flow potential G considered for CDP model is the Drucker-Prager hyperbolic function (Eq. 1):

$$G = \sqrt{(\epsilon \sigma_{t0} \tan \psi)^2 + \bar{q}^2} - \bar{p} \tan \psi \quad (1)$$

where, ψ; the dilation angle measured in the $\bar{p} - \bar{q}$ plane at high confining pressure, σ_{t0}; is the uniaxial tensile stress at failure, and ϵ; eccentricity parameter defining the rate at which the function approaches the asymptote. The flow potential provides that the flow direction is defined uniquely. It is also continuous and

A. Demir, Hakan Ozturk, A. Bogdanovic, M. Stojmanovska, K. Edip

smooth as well. The function asymptotically approaches the linear Drucker-Prager flow potential at high confining pressure stress and intersects the hydrostatic pressure axis at 90°. A family of hyperbolic potentials in the meridional stress plane is demonstrated in Fig. 1 [4].
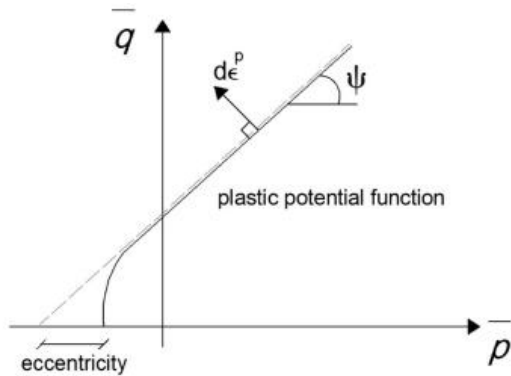

Figure 1. Family of hyperbolic flow potentials in the $\bar{p} - \bar{q}$ plane, [4]

Additionally, dilation angle represents plastic distortion in the damage plasticity model for concrete. ABAQUS software enforces a maximum limit for the value of ψ while constituting CDP material model. It can be calculated via "atan(3/2)" and makes 56.31°.

3. EXPERIMENTAL STUDY

An experimental study performed by Roy and Brena [9] is chosen as a reference study in order to create a numerical model of an RC deep beam. One of the specimens named as DB1.0-0.75L in the reference study is selected as a reference verification specimen. The ratio of shear zone to effective depth of the section (a/d) is 1.0. The specimen geometry, reinforcement, and experimental test setup are demonstrated in Fig. 2. More details about test setup, loading procedure and material properties can be reached in the reference study.
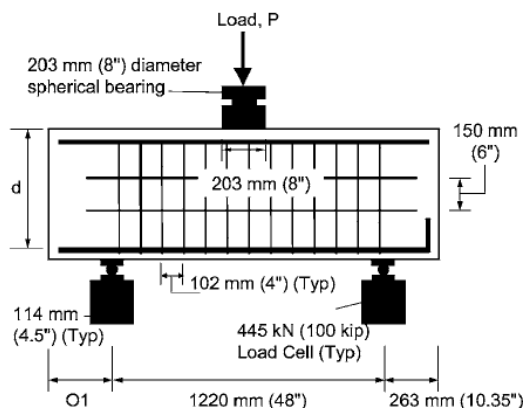
(a) Side view
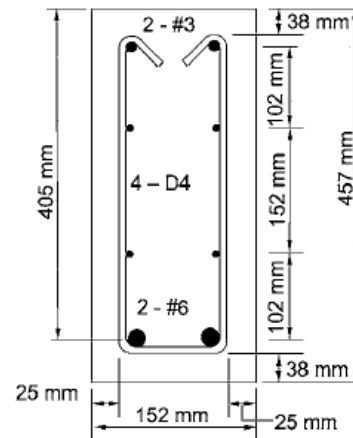
(b) Cross Section

Figure 2. Specimen geometry, reinforcement, and test setup, [9]

Load-displacement result of the test is figured in Fig. 3. Because any tabular data for load-deflection graph were not supplied in the reference study, loads and corresponding displacement values are specified manually [10].
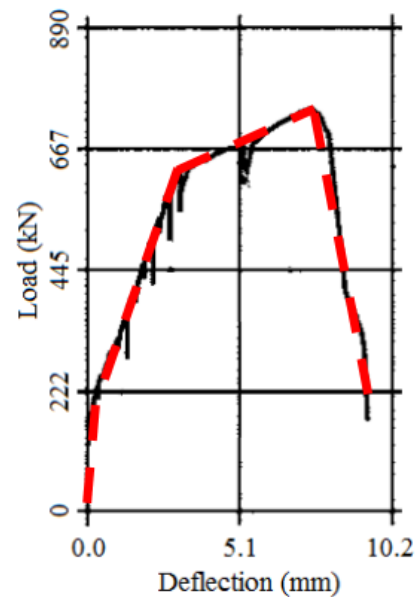

Figure 3. Load-deflection result of the test, [10]

4. NUMERICAL MODELING

In the study, a commercial FE-code ABAQUS/Standard [11] is employed to create numerical simulation. Inelastic behavior of concrete is assigned to FE model by using concrete damaged plasticity (CDP) model. The uniaxial compressive and tensile behaviors of concrete are defined for both pre and post peak stresses. Moreover, in order to consider the degraded response of concrete, two independent uniaxial compressive and tensile

damage variables, dc and dt are defined in the CDP model. Material behavior of reinforcing steel is also defined as elastic and inelastic stress-strain relationships with strain hardening effect.

In order to avoid stress concentration at loading point and supports, steel plates with same dimensions as in the test are added to the FE model. The load is applied as a linear vertical displacement on the loading plate. Supports are considered as a roller and a pin similar to the test.

The element types used in FE model for either of concrete and steel plates are 8-node linear 3D bricks (C3D8R). Moreover reinforcing steel bars are defined as 2-node linear 3D trusses (T3D2). The reinforcement is assumed fully embedded into concrete to take into account the interaction between reinforcement steel and concrete. Additionally, in order to determine more accurate mesh size for the FE model, a parametric study is performed. As a result, an optimum mesh size is determined as 50 mm. General views of the meshed ABAQUS model of reinforcement and concrete are demonstrated in Fig. 4. Because of the fact that similar numerical FE modeling technique of the deep beam described in the study of Demir et al. [10] is utilized, more details can be found in the related study.
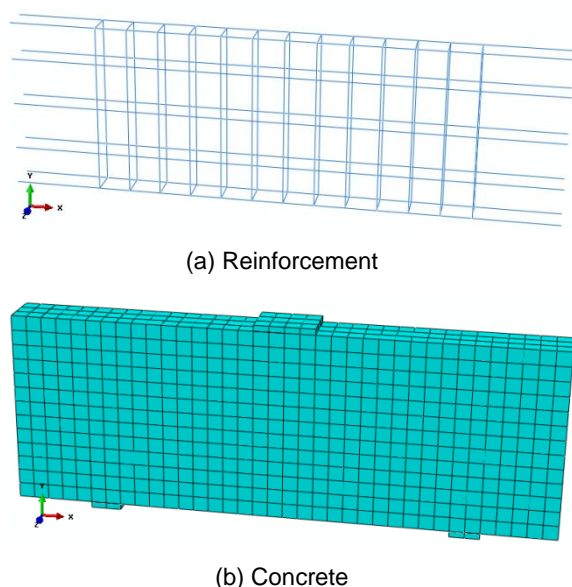

(a) Reinforcement

(b) Concrete

Figure 4. Meshed ABAQUS FE model for reinforcement and concrete, [10]

5. PARAMETRIC STUDY

In order to investigate sensitivity of dilation angle on numerical behavior of an RC deep beam, a parametric study is conducted. For that purpose, four different numerical models are created with varied values of dilation angle tabulated in Table 1. Results of the experimental and numerical studies are compared in terms of load-displacement behavior and ultimate load level (f_u). Deviation percentages from f_u according to the test result are specified as well.

6. RESULTS AND DISCUSSION

The test and numerical study results are presented in Table 1 and demonstrated in Fig. 5. The ultimate load values of the test and numerical models are tabulated, and error of numerical results in f_u are compared with the test result in the table.

Table 1. Results of the experimental and numerical studies

#	Model name	ψ	f_u (kN)	Error % in f_u
1	DB-Test	-	740	-
2	DB-1	20	450	-39.2
3	DB-2	30	490	-33.8
4	DB-3	40	621	-16.1
5	DB-4	56.3	720	-2.7

It can be clearly seen from Fig. 5 that dilation angle plays very important role on numerical simulation results in a way that it changes the numerical load-displacement behavior of a deep beam significantly. The numerical model DB-1, assigned ψ as 20° to FE model, performed very brittle behavior and the deviation from f_u was obtained as 39.2 %. Moreover the model DB-2 exhibited similar behavior like DB-1. Along with the increase in value of ψ, load capacity of the numerical members has started to increase and brittle behavior, however, has remained to be observed. For the last model (DB-4), not only increase in both ultimate load capacity and ductility is experienced but also negligible deviation from the test result is achieved for f_u.
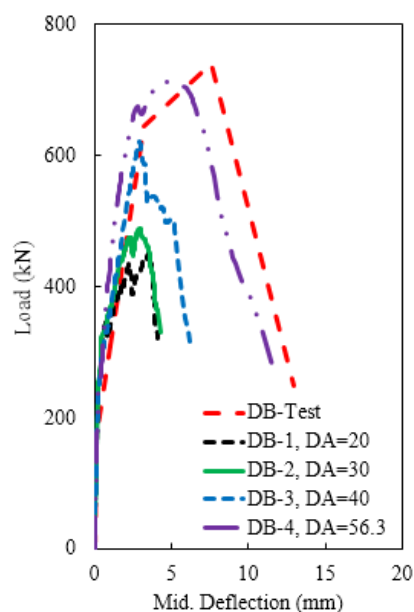
A. Demir, Hakan Ozturk, A. Bogdanovic, M. Stojmanovska, K. Edip

Figure 5. Comparison of load-displacement results

7. CONCLUSIONS

In the present study, a parametric FE study is performed in order to evaluate the effect of dilation angle on numerical simulation of nonlinear behavior of RC deep beams. For this aim, a numerical verification of an existing experimental study of a deep beam is conducted by using ABAQUS software with varied value of ψ defined to the FE models. Results of the experimental and numerical studies are compared in terms of load-displacement behaviors, and error percentage in ultimate load levels according to the test result.

The numerical results are deduced that dilation angle plays very important role on numerical simulation of RC deep beams. A FE model of an RC deep beam assigned very small values of dilation angle exhibits very brittle behavior with very low ultimate load capacity. Along with increase in its value in simulations, not only a significant increase in ultimate load capacity is experienced but also a more ductile behavior is achieved for RC deep beams.

For numerical simulation of an RC deep beam, a proper value for dilation angle should be selected and defined to the FE model. Because of high stiffness and load capacities of deep beams due to its nature, a big value around 50° can be considered for ψ that gives very accurate numerical result in terms of load-displacement behavior. For the values lower than the proposed value, numerical results become distant from test results. Nevertheless, it should be noted that until finding a reasonable value for ψ, a parametric numerical study should be performed with varied values of the parameter in order to achieve more accurate numerical results to simulate nonlinear behavior of RC deep beams.

REFERENCES

[1] N. Caglar, A. Demir, H. Ozturk, and A. Akkaya, "A simple formulation for effective flexural stiffness of circular reinforced concrete columns," Eng. Appl. Artif. Intell., vol. 38, pp. 79–87, 2015.

[2] A. Demir, N. Caglar, H. Ozturk, and Y. Sumer, "Nonlinear finite element study on the improvement of shear capacity in reinforced concrete T-Section beams by an alternative diagonal shear reinforcement," Eng. Struct., vol. 120, pp. 158–165, 2016.

[3] P. Grassl, "Modelling of dilation of concrete and its effect in triaxial compression," Finite Elem. Anal. Des., vol. 40, pp. 1021–1033, 2004.

[4] "ABAQUS online documentation server," Dassault Systèmes Simulia Corp. Providence, RI. [Online]. Available: http://50.16.225.63/v6.14/.

[5] B. Mercan, A. E. Schultz, and H. K. Stolarski, "Finite element modeling of prestressed concrete spandrel beams," Eng. Struct., vol. 32, no. 9, pp. 2804–2813, 2010.

[6] M. Szczecina and A. Winnicki, "Selected aspects of computer modeling of reinforced concrete structures," Arch. Civ. Eng., vol. LXII, no. 1, pp. 51–64, 2016.

[7] Y. Sümer and M. Aktaş, "Defining parameters for concrete damage plasticity model," Chall. J. Struct. Mech., vol. 1, no. 3, pp. 149–155, 2015.

[8] ACI 318-14, Building Code Requirements for Structural Concrete. American Concrete Institute, 2014.

[9] N. C. Roy and S. F. Breña, "Behavior of deep beams with short longitudinal bar anchorages," ACI Struct. J., vol. 105, no. 4, pp. 460–470, 2008.

[10] A. Demir, H. Ozturk, and G. Dok, "3D Numerical Modeling of RC Deep Beam Behavior by Nonlinear Finite Element Analysis," Disaster Sci. Eng., vol. 2, no. 1, pp. 13–18, 2016.

[11] "ABAQUS/CAE 6.13-2 SE." Dassault Systèmes Simulia Corp., Providence, RI.

SJCE

SCIENTIFIC JOURNAL OF CIVIL ENGINEERING